Utilization of Sugarcane Bagasse Ash in the Synthesis of Low-Cost Ceramic Membranes for Malachite Green Dye Separation

Project report submitted to
Visvesvaraya National Institute of Technology, Nagpur
in partial fulfillment of the requirements for the award of
the degree

Master of Technology
in
Chemical Engineering

by

Aashay B. Gaikwad

Roll No. MT23MCL003

under the guidance of

Dr. Shriram S. Sonawane

Department of Chemical Engineering
Visvesvaraya National Institute of Technology
Nagpur 440 010 (India)

June-2025

Utilization of Sugarcane Bagasse Ash in the Synthesis of Low-Cost Ceramic Membranes for Malachite Green Dye Separation

Project report submitted to
Visvesvaraya National Institute of Technology, Nagpur
in partial fulfillment of the requirements for the award of
the degree

Master of Technology
in
Chemical Engineering

by

Aashay B. Gaikwad

Roll No. MT23MCL003

under the guidance of

Dr. Shriram S. Sonawane

Department of Chemical Engineering
Visvesvaraya National Institute of Technology
Nagpur 440 010 (India)

June-2025

© Visvesvaraya National Institute of Technology (VNIT) 2009

Department of Chemical Engineering
Visvesvaraya National Institute of Technology, Nagpur

Declaration

I, Aashay B. Gaikwad, hereby declare that this dissertation titled **"Utilization of Sugarcane Bagasse Ash in the Synthesis of Low-Cost Ceramic Membranes for Malachite Green Dye Separation"** is carried out by me in the Department of Chemical Engineering of Visvesvaraya National Institute of Technology, Nagpur. The work is original and has not been submitted earlier whole or in part for the award of any degree/diploma at this or any other Institution / University.

Aashay B. Gaikwad
Date:

Certificate

This to certify that the dissertation titled **"Utilization of Sugarcane Bagasse Ash in the Synthesis of Low-Cost Ceramic Membranes for Malachite Green Dye Separation**" is submitted by **Aashay B. Gaikwad** in partial fulfillment of the requirements for the award of the degree of **Master of Technology in Chemical Engineering**, VNIT Nagpur. The work is comprehensive, complete and fit for final evaluation.

Dr. Shriram S. Sonawane (supervisor)
Professor,
Dept. of Chemical Engineering,
VNIT, Nagpur

Dr. Ajit P. Rathod (co- supervisor)
Associate Professor,
Dept. of Chemical Engineering,
VNIT, Nagpur

Dr. Kailas Wasewar
Professor
Head of Department of Chemical Engineering
VNIT, Nagpur
Date:

Visvesvaraya National Institute of Technology, Nagpur

Non-Plagiarism Certificate

This is to certify that the M.Tech. Dissertation "**Utilization of Sugarcane Bagasse Ash in the Synthesis of Low-Cost Ceramic Membranes for Malachite Green Dye Separation"** submitted by Aashay B. Gaikwad, Enrolment No. MT23MCL003, ID No. 30796 is original in nature and not copied from any literature material. Due credit has been given to the original researcher wherever referred.

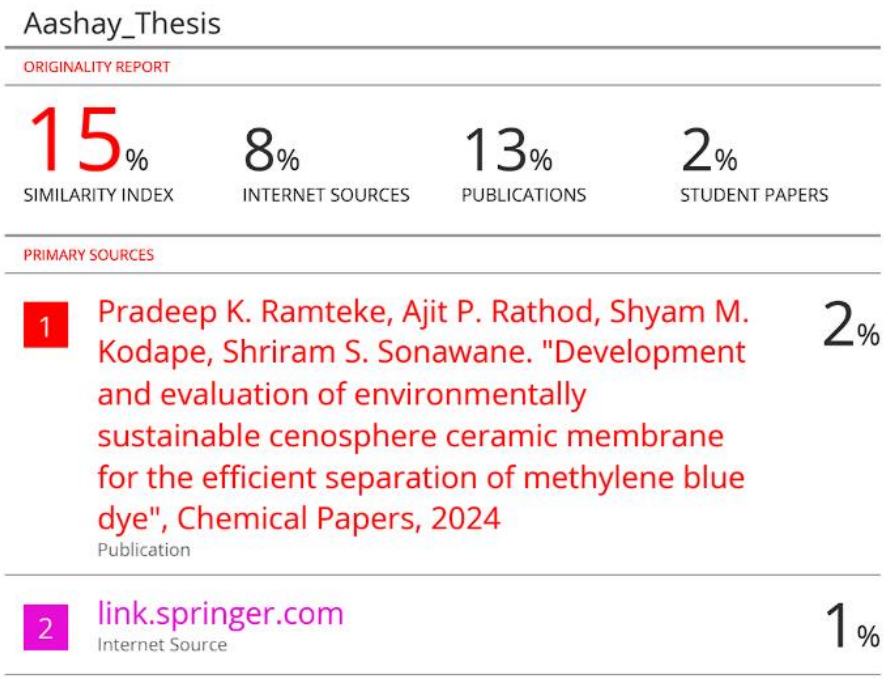

Aashay_Thesis

ORIGINALITY REPORT

15%	8%	13%	2%
SIMILARITY INDEX	INTERNET SOURCES	PUBLICATIONS	STUDENT PAPERS

PRIMARY SOURCES

1	Pradeep K. Ramteke, Ajit P. Rathod, Shyam M. Kodape, Shriram S. Sonawane. "Development and evaluation of environmentally sustainable cenosphere ceramic membrane for the efficient separation of methylene blue dye", Chemical Papers, 2024 Publication	2%
2	link.springer.com Internet Source	1%

Aashay B. Gaikwad

MT23MCL003

Dr. Shriram S. Sonawane
Professor,
Dept. of Chemical Engineering, VNIT,
Nagpur

Acknowledgement

I would like to express my heartfelt gratitude to my research guide, Dr. Shriram S. Sonawane, for his invaluable guidance, constant support, and insightful feedback throughout the course of this thesis. His mentorship has been instrumental in shaping my research and academic development.

I am also deeply thankful to Dr. Ajit P. Rathod, whose expertise, patience, and continuous encouragement played a crucial role in overcoming various challenges during the experimental and analytical phases of my work. Moreover, a special thanks to Mr. Pradeep Ramteke or his continuous support.

I extend my sincere thanks to Dr. Kailas Wasewar, Head of the Department of Chemical Engineering, for providing the necessary infrastructure, resources, and a conducive research environment that greatly contributed to the successful completion of my project.

I am equally grateful to the Department of Chemical Engineering for their academic support and access to facilities, without which this research would not have been possible.

Last but not least, I would like to thank my classmates especially Akshay S. Dorlikar for his constant motivation, constructive discussions, and emotional support throughout this journey.

ABSTRACT

This study reports the development and performance assessment of cost-effective ceramic membranes synthesized from Sugarcane Bagasse Ash (SCBA) and Coal Fly Ash (CFA) for the efficient removal of Malachite Green (MG) dye from industrial effluents. The membrane matrix was formulated by incorporating SCBA and CFA along with inorganic additives such as $CaCO_3$, Na_2CO_3, Na_2SiO_3, and H_3BO_3. The membranes were fabricated via uniaxial pressing followed by sintering at predetermined temperatures (650 °C, 750 °C, and 850 °C) to tailor their microstructural properties. Comprehensive physicochemical characterization, including porosity (via Archimedes' principle), FTIR, PXRD, FESEM-EDS, and chemical resistance tests in acidic and alkaline media, revealed that sintering at 750 °C provided an optimal trade-off between porosity, mechanical integrity, and chemical durability. Water flux analysis indicated peak permeability (0.1139 $L/m^2 \cdot min$) at 650 °C, which declined with higher sintering temperatures due to matrix densification. PXRD and EDS analyses confirmed the formation of crystalline phases such as quartz, mullite, and hematite, which are crucial for structural robustness. The membranes also demonstrated excellent chemical stability, exhibiting less than 1% weight loss in 1 M HCl and NaOH at 850 °C. All membranes achieved high MG dye rejection (>99.78%) under varied pressure and compositional conditions. Additionally, the valorization of SCBA and CFA not only reduces environmental burden but also brings down membrane production costs by up to 40%.

Furthermore, optimization through Response Surface Methodology (RSM) confirmed that a membrane composition with 30% SCBA, sintered at 850 °C under moderate transmembrane pressure, yielded the highest dye removal efficiency. The RSM model exhibited strong predictive accuracy ($R^2 > 0.98$), validating the statistical significance of interaction effects among sintering temperature, SCBA content, and applied pressure on membrane performance. This approach facilitated parameter-level micro-simulation and enabled the design of a membrane system that is both technically robust and statistically optimized for treating dye-contaminated wastewater.

List of Figures

Figure 1 : Chemical structure of malachite green ……...7

Figure 3.1: Size reduction of SCBA using ball mill….……24

Figure 3.2: Pictorial representation of membrane fabrication……..26

Figure 3.3: Experimental setup of dye removal & membrane module…… 26

Figure 3.4: 50 ppm malachite green dye solution…….27

Figure 3.5: Different membranes at different composition and sintering temperature 28

Figure 4.1: Pictorial representation of porosity test ……..……...29

Figure 4.2: Mechanism of pore formation of ceramic membrane……30

Figure 4.3: Effect of sintering temperature, SCBA composition on porosity…….. 31

Figure 4.4: Chemical Resistance of 30% SCBA membrane…….33

Figure 4.5: Water flux at different sintering temperature and pressure ……35

Figure 4.5: Water flux at different sintering temperature and pressure…….37

Figure 4.7: PXRD of 30% SCBA membrane sintered at 750 °C……..39

Figure 4.8: FESEM of 30% SCBA, 750 °C, a)100x b)1000x c)3000x magnified……...40

Figure 4.9: FESEM of 30% SCBA, 850 °C, a)100x b)1000x c)3000x magnified……...41

Figure 4.10: a) selected area, 30% SCBA, 750°C b) EDS elemental composition……..43

Figure 4.11: a) selected area, 30% SCBA, 850°C b) EDS elemental composition ……...44

Figure 4.12: Elemental composition of SCBA Membranes at different sintering temperature……...45

Figure 4.13: Malachite green calibration (stock solution) Curve (λ max = 618 nm)…...46

Figure 4.14: Effect of composition, sintering temperature on dye removal percentage...46

Figure 4.15: Permeate from different membrane at different conditions……..47

Figure 4.16: RSM analysis of membrane at different parameters…….48

List of Tables

Table 2.1: Summary of agro-based membranes for dye removal……22

Table 3.1: General composition for fabricated membrane……...23

Table 4.1: Porosity determination……30

Table 4.2: Effect of HCl & NaOH at pH 1 and pH 14 respectively on membrane……..33

Table 4.3: Water flux of SCBA membrane at different sintering temperature…….34

Table 4.4: Percentage rejection of malachite green of different membrane at different condition……...47

Table of Contents

1. INRODUCTION……...1
   - 1.1 Global Water Crisis & Industrial Pollution…….2
   - 1.2 Emergence of Membrane Technology……3
   - 1.3 The Rise of Ceramic Membranes……3
   - 1.4 Cost Challenges and the Role of Alternative Raw Materials…….4
   - 1.5 Historical Evolution of Membrane Science……5
   - 1.6 Growth of Ceramic Membrane Market & Application…….....5
   - 1.7 Rationale for Selecting Sugarcane Bagasse Ash & coal fly ash as Raw Material for Ceramic Membrane Fabrication……6
     - 1.7.1 Motivation & Background…….....6
     - 1.7.2 Overview of Malachite Green (MG) dye……7
     - 1.7.3 Challenges and Approaches in Malachite Green Removal……8
     - 1.7.4 Regulatory and Environmental Context…….....8
     - 1.7.5 Introduction to Membrane Technology…….....9
     - 1.7.6 Membrane Fabrication Techniques……9
     - 1.7.7 Membrane Properties and Performance Factors……...13
     - 1.7.8 Fouling and Cleaning of Membranes……15
   - 1.8 Mitigation Techniques for Fouling……...16
   - 1.9 Motivation for the Present Study……..17
2. LITERATURE REVIEW……....19
3. MATERIALS & METHODOLOY…….23
   - 3.1 Chemicals Required…….24
   - 3.2 Membrane Fabrication Steps……24
   - 3.3 Experimental Procedure……...26
     - 3.3.1 Dye Removal Testing……...27
     - 3.3.2 Subjecting membrane to the setup……..28
4. RESULTS & DISCUSSION……...29
   - 4.1 Physical & Structural Analysis
     - 4.1.1 Porosity……29
     - 4.1.2 Chemical Analysis……...32

4.1.3 Water Flux……..34
4.2 Characterization
4.2.1 FTIR……...36
4.2.2 PXRD……38
4.2.3 FESEM……...39
4.2.4 EDS……41
4.3 Malachite green dye rejection……46
4.4 Optimization……...48
4.5 Future Outcome……..49
5. CONCLUSION……..51
6. REFERENCES……..52

1. INTRODUCTION

In past years, separation technologies involved in membranes have experienced significant growth because of their high efficiency in achieving effective separations with lower energy consumption and minimal environmental impact. Membrane processes have found numerous applications in industrial sectors, including chemical engineering, pharmaceuticals, food processing, and especially water and wastewater treatment. Amongst the various membrane technologies, ceramic membranes have garnered considerable awareness owing to their higher mechanical strength, chemical resistance, and thermal stability. These characteristics make them potential candidate for harsh environments, such as those encountered in the treatment of industrial effluents, desalination, and mitigation of organic pollutants [1].

The increasing demand for efficient water treatment technologies arises from the deteriorating quality of drinking water, which leads to significant health issues. According to the World Health Organization, waterborne diseases contribute to approximately 1.7 million fatalities annually. As a result of which, the development of sustainable, cost-effective water treatment technologies is a pressing concern [2], [3].

Membrane separation technologies are often regarded as one of the most promising solutions for representing the global water paucity crisis [4]. Ceramic membranes are favoured over polymeric membranes because of their robustness, which is crucial for industries such as textile, pharmaceutical, and chemical processing, where high-temperature and high-pH conditions get into existence [5], [6]. Ceramic membranes offer superior performance, especially in filtration processes for the removal of particulate matter, dyes, and heavy metals from water and wastewater [7].

Natural raw materials like fly ash, rice husk ash, sugarcane bagasse, and cenosphere have been explored for the development of low-cost ceramic membranes [8], [9]. Fly ash, a waste byproduct of coal combustion, has been widely studied for its potential as a precursor for ceramic membranes [10]. Recent studies have put light upon the utilization of fly ash, a lightweight, particles with high silica content, derived from thermal power plant [11]. Fly ash -based ceramic membranes have demonstrated

promising results due to their distinctive structural properties, such as high surface area, porosity, and chemical stability.

The use of waste-derived materials for membrane fabrication not only provides an economical alternative to conventional materials but also promotes environmental sustainability by recycling industrial waste. In addition to fly ash, fly ash has emerged as a novel material in membrane fabrication, offering several advantages, such as ease of processing, good mechanical strength, and high chemical resistance. Various techniques, including uniaxial pressing and sintering at controlled temperatures, have been employed to make fly ash -based ceramic membranes with controlled porosity and permeability [10].

Despite the promising potential, challenges lie in optimizing the properties of these membranes, particularly in controlling pore size, improving flux, and enhancing mechanical stability. The sintering temperature is a critical factor that affects the final properties of the membrane, such as porosity, pore size, mechanical strength, and chemical resistance. Studies have shown that sintering at higher temperatures leads to increased densification, which reduces porosity and permeability. Therefore, understanding the relationship between sintering conditions and membrane performance is crucial for optimizing the fabrication process and achieving membranes with desirable characteristics [12].

1.1 Global Water Crisis and Industrial Pollution

Access to clean drinking water is one of the most pressing global challenges of the 21st century. Increasing population, sudden industrialization, and urbanization have contributed to escalating levels of water pollution, especially from industrial effluents containing synthetic dyes and heavy metals. The textile, leather, food, and cosmetic industries are primary contributors to dye-laden wastewater, which, when discharged untreated, poses significant threats to aquatic ecosystems and human health. The need for sustainable and cost-effective water treatment technologies is, therefore, more critical than ever before [13].

Traditional treatment approaches such as chemical precipitation, adsorption, and biological degradation often suffer from high operating costs, secondary pollution, or inadequate efficiency in removing persistent pollutants like synthetic dyes [14]. Consequently, membrane-based separation techniques have gained attention for their superior separation efficiency, operational simplicity, and eco-friendliness.

1.2 Emergence of Membrane Technology

Membrane filtration technology has become an essential tool for modern wastewater treatment. It offers selective removal of pollutants by using pressure-driven mechanisms that force contaminated water through semipermeable membranes, allowing for size-based or chemical-specific separation of contaminants [15]. Membranes are generally These membranes are typically grouped according to their pore size into four distinct types: microfiltration (MF), ultrafiltration (UF), nanofiltration (NF), and reverse osmosis (RO). Each type offers different separation capabilities and operational requirements.

Microfiltration membranes, with pore sizes ranging from 0.1 to 5 microns, are well-suited for removing larger particulates, bacteria, and dye aggregates. These membranes require relatively low hydrostatic pressure, making them energy-efficient and practical for various applications, including dye removal [16].

1.3 The Rise of Ceramic Membranes

Despite the extensive use of polymeric membranes, their limitations such as poor thermal stability and chemical degradation restrict their application in harsh environments. Ceramic membranes, on the other hand, offer an upper hand in their excellent mechanical strength, resistance to chemicals, and stability at high temperatures make them highly suitable for demanding separation applications. industrial wastewater treatment. Their longevity and performance in extreme conditions have positioned them as strong candidates for replacing polymeric membranes in demanding filtration processes.

Ceramic membranes are also highly versatile, finding use in gas separation, oil-water separation, saline water treatment, and pharmaceutical purification [17]. Their ability to bear high pressures, corrosive media, and elevated temperatures makes them particularly effective for treating dye-contaminated wastewater generated by textile industries.

1.4 Cost Challenges and the Role of Alternative Raw Materials

One of the most significant barriers to the widespread incorporation of ceramic membranes is their high manufacturing cost. Sugarcane bagasse ash (SCBA), an agro-industrial waste from sugar production, is gaining attention as a sustainable raw material for ceramic membrane fabrication due to its high silica content (typically 55–70%) and the presence of other oxides like alumina and iron oxide [18] [19]. This composition imparts mechanical strength and thermal stability to SCBA-derived membranes, making them comparable to conventional ceramic membranes fabricated from expensive synthetic precursors such as pure alumina or zirconia.

From an economic standpoint, SCBA-based membranes offer significant cost advantages. The high cost of raw materials significantly contributes to the overall expense of conventional ceramic membranes used in industrial processes. For instance, α-alumina-based tubular ceramic membranes with average pore sizes between 1000 and 6000 nm can cost between \$500/m² and \$1000/m². Therefore, minimizing production expenses is crucial for enhancing the commercial viability of ceramic membranes. In contrast, membranes fabricated using kaolin—with pore sizes ranging from 550 to 810 nm—have been reported to cost approximately \$220/m². Furthermore, flat-sheet ceramic membranes developed from kaolin and natural clay, offering an average pore size of around 4000 nm, have shown even lower estimated production costs, around \$130/m² [20]. In contrast, using SCBA; a waste product often available at minimal or no cost—can reduce the raw material expenses substantially. SCBA-based ceramic membranes have been produced for as little as \$19–\$50 per m², which is several times cheaper than conventional ceramics and even competitive with polymeric membranes, which generally cost \$30–\$50 per m² but have a much shorter operational lifespan of 3 to 5 years and lower chemical and thermal stability [21], [22].

1.5 Historical Evolution of Membrane Science

The evolution of membrane technology dates back to rudimentary applications involving animal bladders and intestines used as natural membranes [23]. The modern era began with Bechhold's patenting of nitrocellulose membranes in 1907. This innovation led to developments in microfiltration membranes and later to asymmetrical membranes through phase inversion methods introduced by Loeb and Sourirajan [24].

Over the past century, membrane technology has transformed into a cornerstone of industrial water treatment. Membrane-based processes are now capable of handling a broad range of pollutants through various mechanisms such as size exclusion, charge interactions, and hydrophobic/hydrophilic balance. This transition has spurred exponential growth in the global membrane separation market, which is projected to reach $43.14 billion by 2027 [25], [26].

1.6 Growth of Ceramic Membrane Market and Applications

The ceramic membrane market alone was valued at approximately $4.1 billion in 2018 and is projected to expand at a compound annual growth rate (CAGR) of more than exceeding 11% through 2026 [27], [28], [29]. Asia-Pacific, in particular, is witnessing a surge in demand for ceramic membranes, driven by population growth, industrialization, and increased spending on water purification infrastructure [30].

Ceramic membranes are classified into porous and dense types. Porous ceramic membranes typically possess a hierarchical structure comprising a macroporous support, mesoporous intermediate layers, and a microporous top layer that performs the actual separation. This asymmetric configuration offers a balance between mechanical strength and filtration precision [31].

Their resistance to organic solvents, high-temperature operations, and corrosive chemicals makes ceramic membranes suitable for diverse industrial applications, including but not limited to, chemical processing, beverage production, and dye wastewater treatment [32], [33].

1.7 Rationale for Selecting Sugarcane Bagasse Ash & coal fly ash as Raw Material for Ceramic Membrane Fabrication

The selection of appropriate raw materials is pivotal in the development of ceramic membranes, which are widely recognized for their robustness, chemical stability, and effectiveness in water treatment applications. Among various agricultural by-products, sugarcane bagasse ash (SCBA) has risen as a promising candidate for integration into ceramic membranes due to its unique properties, sustainable sourcing, and compatibility with membrane fabrication processes.

1.7.1. Motivation and Background

Sugarcane Bagasse Ash (SCBA) and Coal Fly Ash (CFA) are promising low-cost raw materials for ceramic membrane fabrication due to their high content of silica (SiO_2) and alumina (Al_2O_3), which are important for developing thermally stable ceramic structures. SCBA, a by-product of sugar industry combustion, contains 60–80% amorphous silica along with fluxing agents such as CaO, K_2O, and MgO [34]. CFA, derived from coal-fired power plants, comprises 30–60% SiO_2, 15–35% Al_2O_3, and significant amounts of Fe_2O_3 and CaO [35]. These oxides facilitate vitrification and sintering at relatively lower temperatures (~900–1000 °C), which reduces the energy demand during membrane formation [36]. The thermal decomposition of organic matter in SCBA and the presence of hollow particles (cenospheres) in CFA also promote pore generation, enabling the fabrication of membranes with tunable porosity and high-water flux [34].

Beyond compositional advantages, the integration of SCBA and CFA into membrane production supports circular economy and waste valorization principles [37], [38]. These materials, otherwise treated as solid waste and landfilled, can be transformed into value-added filtration media, mitigating environmental hazards while lowering production costs compared to conventional ceramic powders. Membranes produced from SCBA and CFA exhibit desirable properties such as mechanical strength, acid/base resistance, and stability under harsh operational conditions, making them suitable for dye removal and wastewater treatment [36], [39]. Hence, the use of

SCBA and CFA as raw materials not only enhances the technical viability of ceramic membranes but also addresses broader goals of sustainability and resource efficiency.

1.7.2 Overview of Malachite Green (MG) dye

Malachite Green (MG) is a synthetic triphenylmethane dye ($C_{23}H_{25}ClN_2$) widely used for its vibrant green colour in textile dyeing, aquaculture, and other industrial sectors. Its chemical structure, characterized by aromatic rings and a cationic nature, imparts high solubility and strong affinity for natural fibers such as wool, silk, and cotton, making it a preferred dye in the textile industry. Additionally, MG is valued in aquaculture for its potent antifungal and antiparasitic properties, aiding in the treatment of fish and aquatic organisms [40], [41].

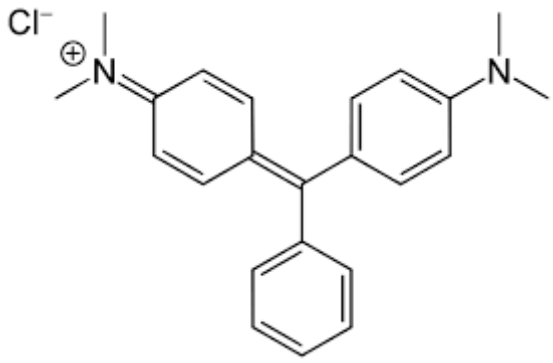

Fig. 1: Chemical structure of malachite green

The necessity for dye separation from wastewater, particularly MG, arises from the significant environmental and health hazards posed by synthetic dyes. Industrial processes, especially in textiles, discharge large volumes of dye-laden effluents-world wide, about 280,000 tons of synthetic dyes enter natural streams annually. MG is notably persistent, displaying high stability, non-biodegradability, and resistance to light and oxidizing agents. Its presence in water bodies not only impairs visual water quality but also disturbs aquatic ecosystems by reducing sunlight penetration, inhibiting photosynthesis, and affecting the physiological functions of aquatic organisms. MG is toxic to various aquatic life forms and can bioaccumulate, leading to deformities, reproductive issues, and mortality in fish and other species [40].

For humans, MG exposure is linked to mutagenicity, carcinogenicity, liver damage, and skin and respiratory irritation. Its metabolic reduction in mammals produces leucomalachite green, a compound associated with increased tumor risk. MG's persistence in sediments (half-life up to 50 days) and its ability to bioaccumulate in the food chain amplify its risk profile, making its removal from wastewater an urgent priority for both environmental and public health protection.

1.7.3 Challenges and Approaches in Malachite Green Removal

Conventional wastewater treatments often fail to adequately remove persistent dyes like MG due to their chemical stability and resistance to biodegradation. This inadequacy necessitates the development and implementation of advanced treatment technologies. Among these, adsorption (using low-cost, recyclable materials), membrane filtration, advanced oxidation, and bioremediation have been explored for MG removal. Adsorption stands out as an effective, economical, and scalable method, with materials such as activated carbon, clays, and nano-composites showing high removal efficiencies. Recent research demonstrates that nano-bentonite, MgO-impregnated clays, and immobilized fungi can achieve MG removal rates exceeding 90%, with optimized operational parameters (pH, temperature, contact time, adsorbent dosage) further enhancing efficacy. These approaches not only address the technical challenge of MG removal but also align with sustainability goals by utilizing natural or waste-derived materials as adsorbents [41].

1.7.4 Regulatory and Environmental Context

Recognizing the risks, regulatory bodies such as the European Union and the US EPA have banned or restricted MG use in food processing and aquaculture. However, enforcement and adoption of safer alternatives and advanced treatment methods remain inconsistent, particularly in developing regions. The ongoing research and innovation in dye separation technologies are thus critical for bridging regulatory gaps and ensuring effective mitigation of dye pollution [42].

1.7.5 Introduction to Membrane Technology

Overview of Membrane Filtration Technologies, Including the Types of Membranes (Microfiltration, Ultrafiltration, Nanofiltration, Reverse Osmosis) and Their Applications in Wastewater Treatment

Membrane filtration technologies are widely used for separating particles, solutes, or gases in various industrial applications, especially in wastewater treatment. The effectiveness of these technologies depends largely on the size of the pores in the membrane and the type of contaminants to be removed. Membranes are typically classified into the following categories:

- **Microfiltration (MF)**: Microfiltration membranes have pore sizes ranging from 0.1 to 10 microns. These membranes are effective in removing big particles, such as suspended solids, bacteria, and algae, from water. MF is commonly used in pre-treatment processes, such as water clarification, and in industries like food and beverage processing.

- **Ultrafiltration (UF)**: Ultrafiltration membranes have smaller pores (typically between 1 and 100 nm) and can remove macromolecules, colloidal particles, and certain bacteria and viruses. UF is commonly used in applications such as water purification and wastewater treatment, especially for separating proteins, emulsions, and other organic materials from liquids.

- **Nanofiltration (NF)**: Nanofiltration membranes operate with pore sizes between 1 and 10 nm and are used for removing smaller organic molecules, divalent ions, and specific salts. NF is commonly applied in water softening and the removal of pesticides and heavy metals from wastewater.

- **Reverse Osmosis (RO)**: Reverse osmosis membranes have the smallest pores (less than 1 nm) and are highly effective in separating salts, heavy metals, and microorganisms from water. RO is widely used for desalination, producing high-purity water from seawater or brackish water, as well as in industrial wastewater treatment.

Membrane filtration is widely recognized for its efficiency and ability to target specific contaminants, offering a sustainable alternative to conventional treatment methods like chemical coagulation or sedimentation [43].

The Importance of Ceramic Membranes, Including Their Advantages Over Polymeric Membranes (e.g., High Thermal Stability, Resistance to Harsh Chemicals)

Ceramic membranes are an important class of filtration membranes, particularly for applications that require robustness under challenging conditions. Ceramic membranes are made from inorganic materials such as alumina, zirconia, and titania. These materials provide several pros over polymeric membranes:

- High Thermal Stability: Ceramic membranes can withstand higher temperatures (up to 1000°C in some cases) compared to polymeric membranes, which often degrade at temperatures above 80°C. This makes ceramic membranes suitable for applications where high-temperature filtration is required, such as in the chemical, food, and beverage industries.
- Chemical Resistance: Ceramic membranes are highly resistant to a wide range of chemicals, including acids, alkalis, and organic solvents. This property makes them ideal for wastewater treatment in industries that produce chemically aggressive effluents, such as textile, pharmaceutical, or petrochemical industries.
- Durability and Lifespan: Ceramic membranes generally have a longer operational lifespan than polymeric membranes. They are less prone to fouling and can be cleaned more effectively, resulting in lower operational and maintenance costs over time [44].

These advantages make ceramic membranes particularly useful for industrial applications that demand consistent performance in harsh conditions.

1.7.6 Membrane Fabrication Techniques

The fabrication of ceramic membranes involves various well-established techniques, each of which has specific advantages depending on the desired membrane properties and applications. Some of the most common traditional ceramic membrane fabrication methods include:

- **Extrusion**: In the extrusion method, a ceramic paste is forced through a mold to form membranes with specific shapes, such as tubular or hollow fiber membranes. This technique is commonly used for producing membranes with uniform thickness and excellent mechanical properties. Extrusion is widely employed in industrial-scale production due to its efficiency and scalability.

- **Tape Casting**: Tape casting involves spreading a slurry of ceramic material onto a substrate and drying it to create thin, flat ceramic sheets. This method is commonly used to produce membranes with a thin, dense structure, which is ideal for high-performance filtration applications. Tape casting is particularly useful for producing large-area membranes with controlled pore structures.

- **Slip Casting**: Slip casting is a process where a slurry or "slip" of ceramic material is poured into a mold, where it hardens and takes the desired shape. It is often used for producing more complex shapes, including tubular and flat membranes, and allows for the precise control of membrane thickness. This technique is useful for producing high-precision membranes, especially for laboratory-scale applications.

Other techniques, such as **isostatic pressing** and **hot pressing**, are also used to fabricate ceramic membranes, but the methods listed above remain the most commonly used due to their established effectiveness in membrane fabrication [45].

Benefits of Low-Cost, Sustainable Alternatives Like Using Agricultural Waste Materials Such as Sugarcane Bagasse Ash

In recent years, there has been increasing interest in sustainable and cost-effective alternatives for ceramic membrane fabrication, such as utilizing agricultural waste materials like sugarcane bagasse ash (SCBA). SCBA is a byproduct of sugarcane processing, and its use in membrane fabrication offers several benefits:

- **Cost-Effectiveness**: Agricultural waste materials like SCBA are typically low-cost or even waste products in many regions where sugarcane is grown. This makes them an attractive alternative to more expensive raw materials like alumina, zirconia, or titania. Using SCBA helps lower the overall cost of membrane production, making ceramic membranes more affordable, especially in developing regions or industries aiming to reduce production costs.

- **Sustainability**: The use of agricultural waste materials such as SCBA promotes **environmental sustainability** by reducing waste disposal issues and minimizing the demand for non-renewable raw materials. SCBA contains **silica** and other compounds that can contribute to the formation of strong, durable ceramic membranes with suitable filtration properties.

- **Waste Valorization**: The use of sugarcane bagasse ash for ceramic membrane fabrication contributes to **waste valorization**, where agricultural byproducts are repurposed into valuable materials. This helps close the loop in industrial waste management and supports a circular economy [46].

The incorporation of sugarcane bagasse ash (SCBA) into ceramic membrane synthesis involves several key methodologies that enable the creation of high-performance membranes while utilizing an agricultural byproduct. These methodologies include several fabrication techniques can be employed to improve the performance of SCBA-based ceramic membranes:

- Co-Firing: Co-firing is a widely used technique that involves firing SCBA along with other raw materials, such as alumina or zirconia, at high temperatures. This process ensures a well-bonded, homogenous structure and helps achieve optimal pore structure and membrane stability. Co-firing also allows for the optimization of the material properties by controlling the firing temperature and atmosphere.

- Sintering: Sintering is a heat treatment process where the ceramic material is heated to a temperature just below its melting point, allowing the particles to fuse together. In SCBA-based membranes, sintering helps improve the mechanical strength and porosity of the material, ensuring that the final membrane is both durable and capable of effective filtration.

- Mixing with Other Raw Materials: To further enhance the performance of SCBA-based membranes, SCBA is often mixed with other raw materials such as alumina, silica, or titanium oxide. This mixing helps improve specific properties such as mechanical strength, thermal stability, and fouling resistance. The inclusion of these materials can help address any weaknesses in SCBA-based membranes and make them more suitable for a wider range of filtration applications.

By employing these fabrication techniques, researchers are able to fine-tune the performance characteristics of SCBA-based ceramic membranes, making them more effective for applications like water treatment and dye removal.

Structural and Performance Analysis of Sugarcane Bagasse Ash-Based Ceramic Membranes, Including Porosity, Flux, and Mechanical Strength

The structural and performance analysis of SCBA-based ceramic membranes is crucial for evaluating their suitability for various applications. Key factors such as porosity, flux, and mechanical strength are essential to determine the membrane's efficiency and durability [46]:

- **Porosity**: Porosity is a critical factor in membrane performance, as it determines the membrane's permeability and its ability to separate specific contaminants. The porosity of SCBA-based ceramic membranes is influenced by the sintering temperature, the particle size distribution, and the presence of other raw materials. Optimal porosity allows for efficient filtration while maintaining structural integrity.

- **Flux**: Flux refers to the rate at which water or other fluids pass through the membrane. High flux is desirable in membrane filtration applications, as it increases the efficiency of the process. The flux of SCBA-based ceramic membranes can be enhanced by controlling the membrane's pore size distribution and surface characteristics. Membranes with the right balance of porosity and surface smoothness tend to have better flux rates.

- **Mechanical Strength**: Mechanical strength is an important property that ensures the membrane can withstand the pressure and mechanical stresses encountered during filtration. SCBA-based ceramic membranes typically exhibit good mechanical strength, especially when sintering or co-firing with stronger materials like alumina. The presence of silica in SCBA contributes to the overall rigidity and durability of the membrane.

1.7.7 Membrane Properties and Performance Factors

Influence of Membrane Composition (e.g., Ratio of Bagasse Ash to Other Components) on Membrane Properties Such as Pore Size, Mechanical Strength, and Filtration Capacity

The composition of sugarcane bagasse ash (SCBA)-based ceramic membranes significantly impacts their pore size, mechanical strength, and filtration capacity, making the selection and ratio of materials crucial to the final membrane performance. The ratio of SCBA to other components, such as alumina, silica, and other inorganic materials, plays a key role in determining the properties of the membrane.

- Pore Size: The pore size of SCBA-based membranes is largely determined by the ratio of SCBA to other materials and the fabrication method used (e.g., sintering or extrusion). A higher proportion of SCBA generally results in larger pores, which can increase permeability but may reduce selectivity for dye or particulate removal. Controlling the ratio of SCBA with other materials allows for tuning the pore size to achieve the desired filtration characteristics for specific applications, such as dye removal.

- Mechanical Strength: The inclusion of materials like alumina or zirconia along with SCBA can enhance the mechanical strength of the ceramic membrane. Higher levels of SCBA provide a low-cost, sustainable base, but they may need to be combined with stronger materials to ensure the membrane can withstand the physical stress of filtration, especially under high pressure. Properly balancing the composition of SCBA and other raw materials is essential for optimizing the mechanical properties of the membrane, ensuring its durability and longevity.

- Filtration Capacity: The filtration capacity of SCBA-based ceramic membranes is directly influenced by their porosity and structural integrity. The correct balance between SCBA and other materials contributes to achieving the right combination of high flux (water permeability) and high rejection efficiency for dyes and contaminants. Membranes with smaller pores, achieved by optimizing material ratios, typically have higher rejection rates but may exhibit lower flux, so adjusting the composition is crucial for optimizing both properties for specific industrial needs.

The use of sugarcane bagasse ash (SCBA)-derived ceramic membranes for dye removal from industrial effluents has been extensively studied due to the increasing environmental concerns associated with the discharge of synthetic dyes into water bodies. Dyeing industries, such as those in textiles, food processing, and pharmaceuticals, produce large

volumes of effluents containing harmful dyes that can cause environmental pollution and pose health risks to humans and aquatic life. SCBA-based ceramic membranes are seen as a promising solution to treat such effluents due to their cost-effectiveness, high performance, and environmental sustainability.

Research has shown that SCBA-derived ceramic membranes [47] can effectively remove a wide range of dyes from wastewater, including Malachite Green, Methylene Blue, and Rhodamine B. The high silica content of SCBA enhances the membrane's structural integrity, while its chemical and thermal stability make it a suitable material for removing dye pollutants from industrial effluents. These membranes can selectively adsorb dye molecules while allowing clean water to pass through, making them an attractive option for wastewater treatment systems.

1.7.9 Fouling and Cleaning of Membranes

Membrane fouling is a major issue in filtration processes, especially in ceramic membrane applications for dye removal and wastewater treatment. Common fouling problems that affect the performance of ceramic membranes, including those derived from sugarcane bagasse ash (SCBA), include [48]:

- Dye Accumulation: In applications like dye removal from textile wastewater, dyes can stockpile on the membrane surface, forming a cake layer that obstructs the flow of water. This layer increases the membrane resistance, reducing flux and causing operational inefficiencies. The accumulation of dye molecules can also lead to irreversible fouling if not adequately managed.

- Scaling: Scaling occurs when inorganic salts (e.g., calcium carbonate, calcium sulfate) precipitate on the membrane surface due to changes in temperature, pH, or concentration. This can significantly reduce the membrane's permeability and efficiency. In SCBA-based ceramic membranes, which are often exposed to high-salinity feed solutions, scaling is a common issue that can hinder performance and necessitate frequent maintenance.

- Biofouling: Biofouling occurs when microorganisms, such as bacteria, algae, or fungi, adhere to the membrane surface and form biofilms. These biofilms block the membrane pores, leading to a significant drop in flux and filtration efficiency.

Biofouling is particularly problematic in wastewater treatment, where organic matter and nutrients promote microbial growth on the membrane surface.

1.8 Mitigation Techniques for Fouling

To minimize fouling and enhance the performance of SCBA-based ceramic membranes, several mitigation strategies can be employed [49]:

- Membrane Surface Modifications: One effective method for reducing fouling is through surface modifications that enhance the hydrophilicity of the membrane surface. Hydrophilic coatings or functional groups (such as hydroxyl or carboxyl groups) can be grafted onto the membrane surface to reduce the affinity between the membrane and contaminants like dyes, proteins, or microorganisms. This makes it more difficult for fouling agents to adhere to the membrane, improving anti-fouling properties.

- Cleaning Protocols: Regular and effective cleaning is crucial for maintaining membrane performance. For SCBA-based ceramic membranes, cleaning protocols typically include both physical cleaning (e.g., backwashing, scrubbing) and chemical cleaning (e.g., using acids, alkalis, or surfactants). Chemical cleaning helps dissolve scale, remove organic fouling, and restore membrane permeability. Physical cleaning, especially backwashing, helps dislodge accumulated foulants from the membrane surface, reducing the buildup of cake layers and extending the membrane's lifespan.

- Membrane Modifications for Anti-Scaling: In addition to surface modifications, anti-scaling coatings can be applied to SCBA-based ceramic membranes to prevent the deposition of inorganic salts. These coatings reduce the likelihood of scaling, maintaining the integrity and efficiency of the membrane in high-salinity conditions.

Long-Term Stability and Reusability of These Membranes in Real-World Conditions

The long-term stability and reusability of SCBA-based ceramic membranes are important considerations for their practical application. Due to their inherent thermal and chemical stability, SCBA-based membranes exhibit strong performance in harsh operational environments, including high temperatures and chemically aggressive feed solutions.

However, maintaining their stability and reusability over extended periods requires effective fouling management strategies, as previously discussed.

Research has shown that SCBA-based ceramic membranes can maintain high performance even after several cycles of fouling and cleaning, provided that appropriate cleaning protocols and surface modifications are employed. The ability to restore membrane performance through cleaning reduces operational costs and makes these membranes a sustainable choice for long-term use in wastewater treatment and dye removal applications.

In real-world conditions, SCBA-based ceramic membranes demonstrate excellent reusability and durability when subjected to frequent cleaning, periodic maintenance, and proper operational conditions. The combination of cost-effectiveness, environmental benefits, and long-term stability positions SCBA-based ceramic membranes as a promising alternative to traditional polymeric and commercial ceramic membranes in various industrial filtration processes [50].

1.9 Motivation for the Present Study

Considering the environmental and economic pressures associated with dye-contaminated wastewater and high-cost filtration materials, this study aims to develop and evaluate a novel ceramic membrane synthesized from sugarcane bagasse ash. Malachite green, a commonly used cationic dye with known toxicity, has been selected as the model pollutant due to its persistence in aquatic environments and resistance to conventional treatment methods. Malachite Green (MG) dye represents a significant environmental challenge due to its persistence, bioaccumulation potential, and toxicity to aquatic ecosystems and human health. Conventional wastewater treatments often fail to remove MG efficiently, necessitating advanced separation technologies. Ceramic membranes fabricated from Sugarcane Bagasse Ash (SCBA) and Coal Fly Ash (CFA) offer a technically robust and sustainable solution by leveraging synergistic material properties for enhanced dye removal. For humans, long-term exposure to Malachite Green is linked to several health risks, including carcinogenicity, liver damage, and skin irritation. Studies have shown that the dye is capable of accumulating in the tissues of humans and animals, leading to

increased health risks with prolonged exposure. This bioaccumulation is concerning because it allows the dye to enter the food chain, with higher concentrations being passed through trophic levels [51], [52].

Sugarcane bagasse ash (SCBA) and coal fly ash (CFA) represent significant environmental liabilities globally and in India, where unmanaged SCBA from sugar mills is often openly burned, releasing particulate matter ($PM_{2.5}$/PM_{10}) and volatile organic compounds (VOCs) that degrade air quality and exacerbate respiratory diseases [53]. In India alone, cities like Nagpur generate ~337,000 kg/month of bagasse waste, clogging water bodies and contaminating soil. Similarly, CFA from coal power plants—India produces ~226 million tons/year—leaches heavy metals (e.g., arsenic, lead) into groundwater and causes silicosis in nearby communities [54], [55]. Only 70% of CFA is utilized nationally, with the rest landfilled, while 40% of India's 1.5–2 million tons of annual bagasse waste is discarded.

Leveraging SCBA (60–80% SiO_2) and CFA (30–60% SiO_2, 15–35% Al_2O_3) for ceramic membrane fabrication converts these pollutants into high-value water purification tools [56]. SCBA's fluxing agents (CaO, K_2O) enable sintering at 900–1000°C-20–25% lower than conventional methods-reducing energy consumption and CO_2 emissions. The hierarchical pore structure, derived from SCBA's organic decomposition and CFA's cenospheres, achieves >90% rejection of toxic dyes like Malachite Green while maintaining high water flux (120–200 $L/m^2 \cdot h \cdot bar$) [57]. Chemically modified SCBA further enhances dye adsorption via electrostatic interactions, reaching 89% removal efficiency. This synergy transforms 280,000+ tons/year of waste into membranes, cutting production costs by 30–40% versus virgin materials [58]. This waste valorization directly mitigates environmental hazards: diverting SCBA from open burning reduces PM/VOC emissions, while repurposing CFA prevents heavy metal leaching. In India, scaling this approach could remediate ~1.5 million tons of agro-industrial waste annually, aligning with circular economy principles. The membranes enable efficient treatment of dye-laden industrial effluents, advancing SDG 6 (Clean Water) by removing persistent contaminants like Malachite Green. Concurrently, low-temperature sintering supports SDG 13 (Climate Action) by curtailing CO_2 emissions [59].

2. LITERATURE REVIEW

Clarissa et al.,2025 stated that Sugarcane bagasse ash (SCBA), a by-product of agro-industrial processes, has emerged as a promising and sustainable raw material for fabricating ceramic membranes, particularly for microfiltration applications. Recent investigations have explored the integration of kaolin with different SCBA loadings (40 wt% and 60 wt%) to produce ceramic membranes aimed at treating crude biodiesel wastewater. Among the compositions studied, the membrane containing 40 wt% SCBA—utilized without any pretreatment—demonstrated optimal performance characteristics. It exhibited a porosity of 38.5%, an average pore size of 0.9 μm, and mechanical strength reaching 27 MPa, effectively balancing permeability with structural integrity. In terms of filtration performance, this membrane achieved notable results, removing up to 83% of color and reducing turbidity by 67%, indicating its efficiency in eliminating suspended and colloidal matter. Microstructural evaluations confirmed the presence of a mesoporous framework conducive to enhanced filtration efficiency. Other membrane variants, containing higher SCBA content, displayed pore sizes in the range of 3.6 μm to 9.5 μm and porosity levels between 56% and 57%, with SCBA contributing significantly as a pore-forming agent. These outcomes highlight the potential of SCBA-based ceramic membranes as low-cost, eco-friendly solutions for treating industrial effluents, especially those from biodiesel production [60].

Dalai et al. (2016) explored Cost-effective approaches have been explored for the removal of iron and manganese from groundwater, notably through the use of activated carbon derived from rice husk (RHAC) and sugarcane bagasse (SBAC). Iron and manganese are commonly found in groundwater, and although their presence in drinking water is not inherently harmful, high concentrations can lead to issues such as discoloration, staining, turbidity, bad taste, and the accumulation of iron oxide or manganese dioxide in pipes. The findings revealed that a soil depth of 50 cm maintained an optimal infiltration rate without any impact from suspended solids, and both RHAC and SBAC were able to remove 100% of iron and manganese from the water after filtration through these soil columns. The results demonstrated that the Budhabalanga river soil had the highest infiltration rate at a depth of 50 cm, emphasizing the importance of studying infiltration rates prior to filtration experiments. Additionally, both RHAC and SBAC showed promising results when placed at the centre of the soil column. The study concluded that further improvements are

necessary for low-cost technologies to enable their widespread use, particularly for communities in need of affordable water filtration solutions. A detailed investigation was conducted to evaluate the influence of key operational parameters—such as initial metal ion concentration, biosorbent dosage, pH, and contact duration—on the efficiency of chromium adsorption. The study employed both native and immobilized sugarcane bagasse as biosorbents to remove Cr(III) and Cr(VI) from synthetic and actual tannery wastewater samples. Results demonstrated that immobilized sugarcane bagasse displayed superior adsorption performance, achieving maximum removal efficiencies of 80.6% for Cr(VI) and 41.5% for Cr(III). Under optimized conditions, a chromium removal efficiency of 73% was attained for real tannery effluent. The findings further emphasized that biosorption capacity was significantly affected by variations in pH, biosorbent dosage, metal ion concentration, and contact time. Equilibrium data were best described by the Langmuir isotherm model, indicating monolayer adsorption behavior, while the kinetic analysis followed a pseudo-second-order model, confirming chemisorption as the rate-limiting step. The findings indicate that immobilized sugarcane bagasse pith can be a highly effective biosorbent for chromium removal in both simulated and real tannery wastewater, showing superior performance compared to other agricultural waste biomasses reported in literature [61].

Xuejing et al. (2021) synthesized a SB-barium carbonate composite, leveraging barium carbonate's affinity for MG to enhance adsorption capacity [62]. Ariani et al. (2018) functionalized SB with phthalate anhydride, introducing carboxylic groups that achieved 121.94 mg/g MG adsorption at pH 4 via electrostatic attraction[63].

Jha et al. (2021) colleagues developed a low-cost ceramic membrane using raw coal fly ash as the primary material, without requiring high-purity additives or commercial ceramics. Their work focused on optimizing sintering temperatures and membrane thickness to attain suitable porosity and mechanical stability. The resulting membrane structure exhibited mesoporous characteristics, crucial for separating larger organic molecules like Malachite Green dye. The membranes showed over 94% dye rejection efficiency, which was attributed to both size exclusion and electrostatic interactions, as the negatively charged membrane surface repelled the cationic dye molecules. Furthermore, their membranes demonstrated strong chemical resistance in acidic and basic environments, as well as flux recovery after multiple reuse cycles, indicating good anti-

fouling performance. This study highlighted the practical and scalable potential of fly ash-derived membranes for dye-laden wastewater treatment, supporting waste valorization and green engineering [64].

Rao et al. (2020) and co-workers investigated the development of porous ceramic membranes from fly ash, with the aim of achieving high mechanical durability and filtration efficiency for wastewater treatment. They studied the effect of fluxing agents (such as borax and feldspar) and sintering at various temperatures (800–1000 °C) on the membrane's porosity, permeability, and mechanical strength. Their optimized membrane demonstrated enhanced hydrophilicity and robust structure, enabling stable permeate flux under operational conditions. When applied to dye-contaminated water, the membranes achieved significant removal of cationic dyes like Malachite Green, owing to the synergistic effects of adsorption and filtration mechanisms. The authors also emphasized the eco-friendly nature of the process, as it repurposes fly ash—a hazardous solid waste—into a value-added filtration material. Their findings contribute to the field by proving that performance-competitive membranes can be fabricated from waste materials using low-energy methods [65].

This study focuses on the utilization of novel sugarcane bagasse ash (SCBA) and coal fly ash (CFA) hybrid membranes represents a technically superior approach for malachite green (MG) dye removal due to synergistic material properties and enhanced separation mechanisms by evaluation of physical and chemical properties. Calculation for the removal of dye also suggested that the novel sugarcane bagasse ash and coal fly-ash based membrane sintered at 650 °C, 750°C, 850°C showed improvement of dye removal of 97-99%.

From the table 2.1, and literature review it is clear that novel raw materials are being a hot topic for dye separation purposes, but there is a very little research for utilizing combination of agricultural and industrial waste into membrane dye separation (malachite green) with dye rejection achieving 99% without application of any external coating.

Table 2.1: Summary of agro-based membranes for dye removal

Type of Membrane	Shape	Dye	Removal (%)	Reference
Coffee Husk Ash	Flat sheet	Congo Red	91–95%	Thakur et al., 2024
Groundnut Shell Ash	Disc	Crystal Violet	89–93%	Bose et al., 2023
Wheat Straw Ash	Flat sheet	Methyl Orange	80–90%	Verma et al., 2022
Cenosphere (Fly Ash-derived)	Flat sheet	Methylene Blue	90–94%	Singh et al., 2022
Orange Peel Ash	Tubular	Acid Orange 7	82–89%	Roy et al., 2022
Peanut Shell Ash	Disc	Rhodamine B	85–92%	Sharma et al., 2021
Corn Cob Ash	Tubular	Reactive Black 5	89–94%	Patel et al., 2021
Sugarcane Bagasse Ash (SCBA)	Disc	Malachite Green	94–98%	Jha et al., 2021
Coal Fly Ash	Disc	Malachite Green	92–96%	Jha et al., 2021
Tea Waste Ash	Flat sheet	Reactive Yellow 145	79–85%	Iqbal et al., 2021
Soybean Husk Ash	Disc	Brilliant Green	84–90%	Nair et al., 2020
Rice Husk Ash (RHA)	Tubular	Methylene Blue	90–95%	Kumar et al., 2020
Pineapple Peel Ash	Flat sheet	Direct Red 80	86–90%	Das et al., 2020
Banana Peel Ash	Disc	Crystal Violet	87–91%	Ali et al., 2020
Coconut Shell Powder	Flat sheet	Congo Red	88–93%	Reddy et al., 2019
Palm Kernel Shell Ash	Disc	Basic Blue 41	83–88%	Mehta et al., 2019

Objectives: a) Fabrication of sugarcane bagasse ash and coal fly ash based ceramic membrane. b) Physical, chemical testing & characterization of the fabricated membrane. c) Determination of percentage rejection of this fabricated membrane for malachite green dye rejection. d) Optimization of the fabricated membrane based on various parameters.

3. MATERIALS & METHODOLOGY

3.1 Chemicals Required

The coal fly-ash, which is the main contributor for air and water pollution, was sourced from the waste generated from thermal power plant, koradi, Nagpur (M.H.). The other component which is sugarcane bagasse ash (SCBA) was procured from a local jaggery mills from amla, MP, India.

The raw materials employed for the fabrication of the green ceramic membrane included calcium carbonate ($CaCO_3$), sodium carbonate (Na_2CO_3), and boric acid (H_3BO_3), all of which were sourced from Thermo Fisher Scientific India Pvt. Ltd., Mumbai. Sodium metasilicate (Na_2SiO_3), serving as the primary binder in membrane formulation, was procured from Loba Chemie Pvt. Ltd. Additionally, analytical-grade hydrochloric acid (HCl) and sodium hydroxide (NaOH) pellets—used for conducting chemical stability tests—were also obtained from Thermo Fisher Scientific. Malachite green dye ($C_{23}H_{25}ClN_2$), supplied by Merck Life Science Pvt. Ltd., Mumbai, was utilized to prepare synthetic dye solutions for performance evaluation. All dye solutions were prepared using distilled water. The experimental procedure was referred from Ramteke et al. (2024) [66].

Inorganic Additives: Calcium carbonate ($CaCO_3$) as a pore-forming agent, Sodium carbonate (Na_2CO_3) for homogeneity, Boric acid (H_3BO_3) to enhance mechanical strength via metaborate formation, Sodium metasilicate (Na_2SiO_3) as a binder.

Initially, the raw sugarcane bagasse ash (SCBA) material was crushed using an Eloquent ball mill. The raw material preparation involved mechanical grinding using a planetary ball mill (HBS Technologies), as shown in Fig. 3.1. The milling process was carried out for 1 hour at a rotational speed of 250 rpm, utilizing a balanced combination of tungsten carbide and zirconia balls with diameters of 3 mm, 5 mm, and 10 mm. This process effectively reduced the average particle size to approximately 0.6 µm. Particle size distribution was determined using Dynamic Light Scattering (DLS) analysis, performed with a Zetasizer Nano instrument (Malvern, UK). In this study, fly ash obtained from a local thermal power plant was washed and directly utilized in membrane formulation through uniaxial hydraulic pressing. The ceramic membrane was synthesized by blending SCBA (sugarcane bagasse ash) and coal fly ash with additional precursors such as calcium

carbonate ($CaCO_3$), sodium carbonate (Na_2CO_3), boric acid (H_3BO_3), and sodium metasilicate (Na_2SiO_3). All components were accurately measured using an analytical weighing balance prior to further processing.

Table 3.1: General composition for fabricated membrane

Chemical/ Material	Weight (gms)	Weight %
Ash (SCBA+ Coal FA)	22.8	76
CaCO3	1.8	6
Na2CO3	1.8	6
H3BO3	1.2	4
Na2SiO3	2.4	8
Total	30	100

Fig 3.1: Size reduction of SCBA using ball mill

3.2 Membrane Fabrication Steps

- **Mixing and Grinding:** Crushing of the bagasse ash using a planetary ball mill (250 rpm, 1 hour) to get fine particle size about 0.6 µm for uniformity. All raw materials were weighed in appropriate proportions as mentioned in the table and thoroughly ground using a mortar and pestle. Additionally, water was introduced

gradually in a dropwise manner to ensure a consistent semi-moist powdery texture. Mixing was done for 10 minutes before and after addition of distilled water.

- **Moulding and Pressing:** The processed mixture was loaded into a metallic mould containing a base disc of 6 cm diameter. The mould was then closed and subjected to uniaxial hydraulic pressing using a hydraulic press (Kimaya Engineers) at a pressure of 150 kgf/cm² for a duration of 10 minutes. The resulting structure, referred to as the green membrane, was carefully removed and allowed to rest at ambient room temperature for 15 hours to stabilize the structure and avoid thermal stress.

- **Drying:** Post stabilization, the green membrane was transferred to a dry air oven (Model No. BTI-29, Bio Technics India) and dried at 50 °C for 6 hours to eliminate residual moisture.

- **Sintering:** The dried membrane was then placed in a muffle furnace (Model No. BTI-36, Bio Technics India). The sintering protocol was initiated by gradually increasing the furnace temperature from ambient to 100 °C over a period of 15 hours to avoid thermal shock. Thereafter, the temperature was further ramped up at a rate of 150 °C per hour until a final sintering temperature of 950 °C was reached. This temperature was held constant for 9 hours to complete the sintering cycle.

- For comparative analysis, membranes were also sintered at 650 °C, 750 °C, 850 °C, and 950 °C using the same thermal ramping strategy. Visual inspection and characterization were conducted to observe structural evolution pre- and post-sintering.

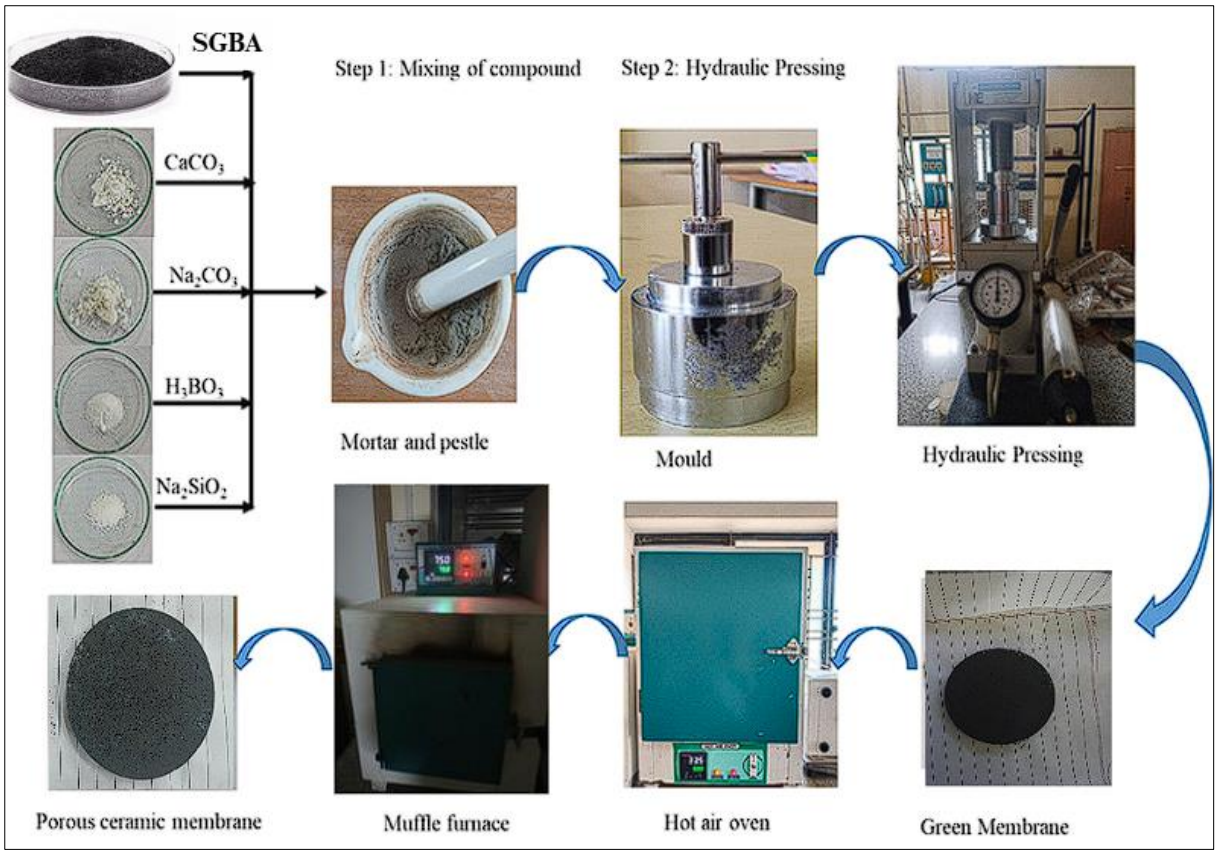

Fig 3.2: Pictorial representation of membrane fabrication

3.3 Experimental Procedure

3.3.1 Dye Removal Testing:

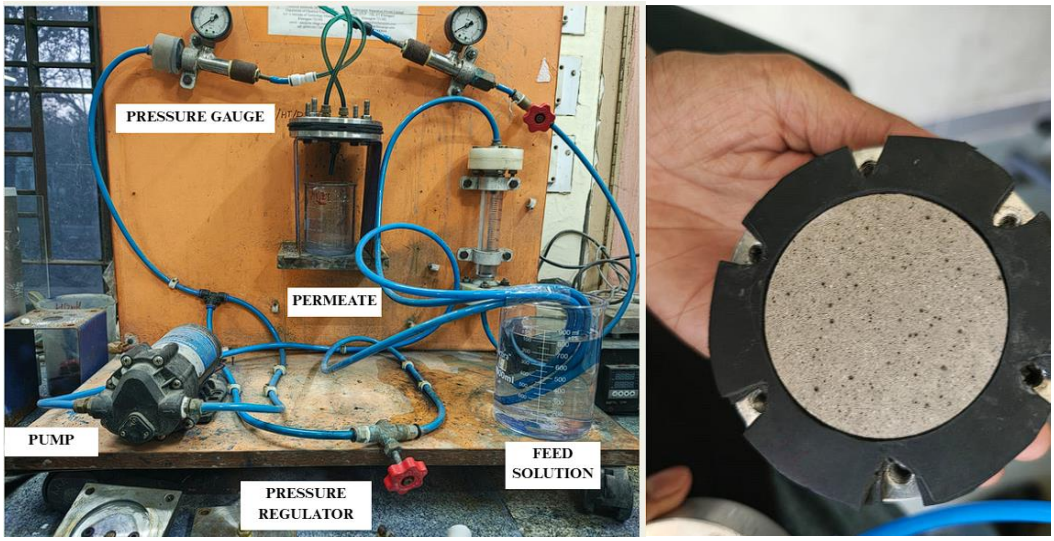

Fig 3.3: Experimental setup of dye removal & membrane module

❖ **Preparation of 50ppm malachite green solution**

Treating malachite green (MG) at a concentration of 50 ppm is technically justified and industrially relevant due to its frequent occurrence in effluents from textile dyeing, leather tanning, paper, and aquaculture industries, where poor dye fixation and discharge practices can result in high dye loads [67]. Moreover, MG is known to degrade into leucomalachite green, a persistent and carcinogenic derivative[67]Several studies employ 50 ppm concentrations to assess the performance and fouling resistance of membrane and adsorbent systems under high-strength dye loading[68], making it a representative stress-test condition. For ceramic membranes, particularly those derived from waste ashes like SCBA, targeting MG removal at 50 ppm allows for realistic performance benchmarking and validates their applicability in treating high-strength industrial wastewater prior to discharge or reuse.

- ❖ **Weighing**: Accurately weigh 50.0 mg of malachite green oxalate using an analytical balance. Use a clean, dry glass vial or watch glass to avoid moisture adsorption.
- ❖ **Dissolution**: Transfer the dye into a 100 mL volumetric flask. Add about 50 mL of DI water and stir until the dye fully dissolves. This yields a 500 ppm intermediate stock solution.
- ❖ **Dilution:** From the intermediate solution, pipette 10 mL into a 100 mL volumetric flask and dilute to the mark with DI water. This yields a 50 ppm working solution.

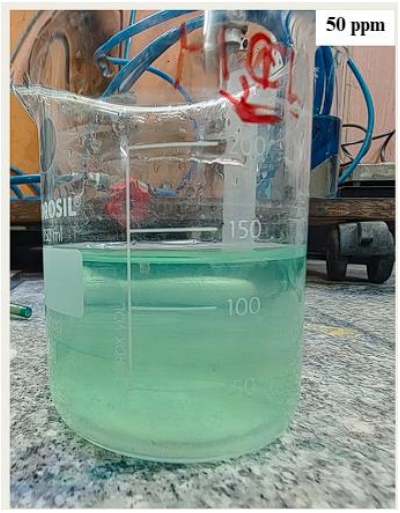

Fig 3.4: 50 ppm malachite green dye solution

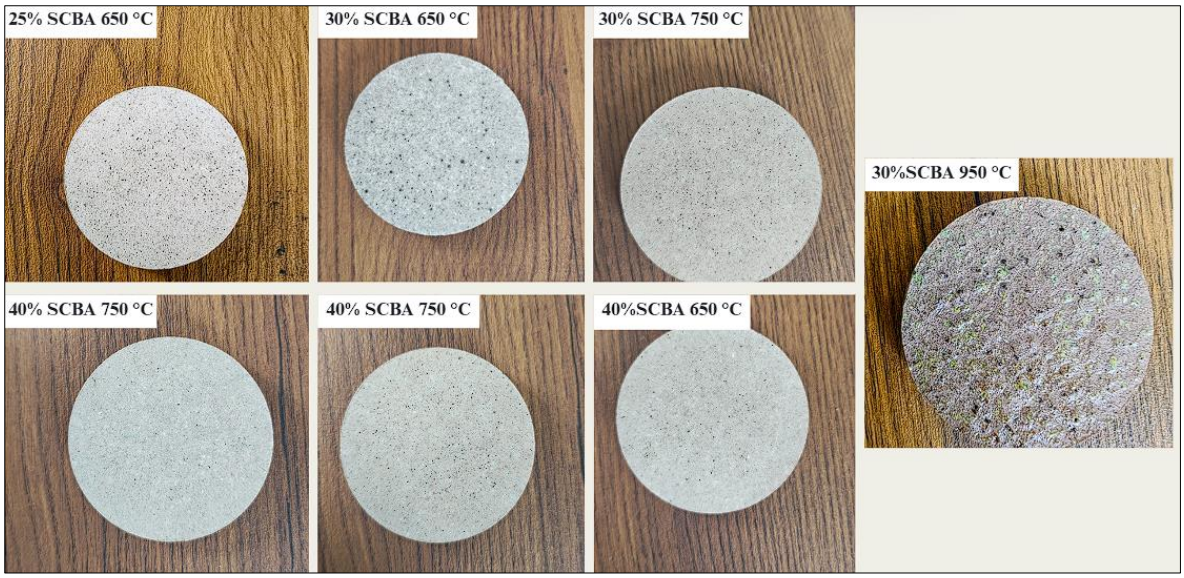

Fig 3.5: Different membranes at different composition & sintering temperature

3.3.2 Subjecting membrane to the experimental setup

- Attaching the membrane to the cross-flow mould in the experimental setup.
- Placing the feed solution and starting the dye removal setup by adjusting the different membranes, at different transmembrane pressure.
- Collection of the permeate and determining the concentration using UV-vis. Spectroscopy.
- Calculation of percentage removal of the dye.

4. RESULTS & DISCUSSION:

4.1 Physical and Structural Analysis:

4.1.1 Porosity: Measured via Archimedes' principle.

Porosity is a key parameter in determining the performance of membranes, particularly in filtration applications. It refers to the fraction of the membrane's volume that is occupied by void spaces or pores, which play a critical role in allowing fluid to pass through while retaining certain particles. High porosity often indicates a membrane's capacity to allow greater fluid flow, but an optimal balance between porosity and mechanical strength is essential for efficient filtration. The calculation of porosity is typically done using the Archimedes principle. In this process, the membrane is first dried at 100°C for one hour to obtain its dry weight (W_d). Next, the membrane is submerged in distilled water for 24 hours, allowing it to absorb water into its pores.

Fig 4.1: Pictorial representation of porosity test

After removing the excess water from the membrane's surface, the wet weight (W_w) is measured. The porosity is then determined by comparing the dry and wet weights of the membrane. This method provides insight into

$$Porosity\ (\%)\ \ \varepsilon = \frac{(w_w - w_d)}{\rho_{water}} * \frac{100}{V_{memb}} \qquad (1)$$

the membrane's ability to retain water, which directly correlates with its potential in various applications such as wastewater treatment, desalination, and filtration processes.

Accurate porosity determination is crucial for optimizing membrane performance, ensuring the desired permeability, and achieving effective separation.

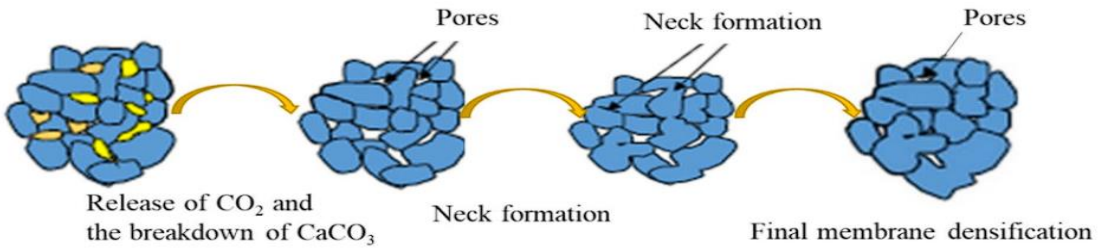

Fig 4.2: Mechanism of pore formation in ceramic membrane (Saikia et al. 2019)

Pore size of ceramic membrane was estimated theoretically using the Guerout–Elford–Ferry Eq. [69], [70].

$$Pore\ size = \sqrt{\frac{(2.9-1.75\varepsilon)*8\eta lQ}{\varepsilon A \Delta P}} \qquad (2)$$

where ε is porosity, Q is the volume of permeate in m3/s, (7) is the viscosity of water at 25°C which equals 8.9 × 10− 4 Pa s, and ΔP is the operational pressure, which is 1 bar and *l* represents the thickness of membrane.

Table 4.1: Porosity determination

%SCBA	Sintering Temp (°C)	W_d (g)	W_w (g)	Avg.t_m (cm)	Dia. (cm)	Porosity (%)
25	650	23.064	29.32	0.620	5.87	37.46
25	750	23.854	28.56	0.595	5.98	28.29
25	850	20.892	20.89	0.623	6.12	16.21
30	650	24.993	24.99	0.632	5.934	24.16
30	750	25.122	25.12	0.627	6.015	19.39
30	850	25.057	25.06	0.619	6.059	15.40

The membrane sintered at 650 °C demonstrated the highest porosity in comparison to the one sintered at 750 °C. This behavior can be attributed to the thermal decomposition of

calcium carbonate ($CaCO_3$) between 540 °C and 760 °C during the sintering process, which results in the formation of calcium oxide (CaO) and the release of carbon dioxide (CO_2). The evolution of CO_2 gas promotes pore formation within the membrane matrix. However, as the sintering temperature increases beyond this range, the membrane enters a densification phase, which leads to a reduction in porosity due to particle fusion and pore closure [71].

Later, cenosphere particles inside the fly ash develop neck structures, a common sintering feature it reduces the amount of pores. It could be credited to the fact that % porosity reduced drastically by 57% in case of 25% SCBA ash from 650°C to 850 °C and 37% in case of 30% SCBA ash from the 650°C to 850°C.

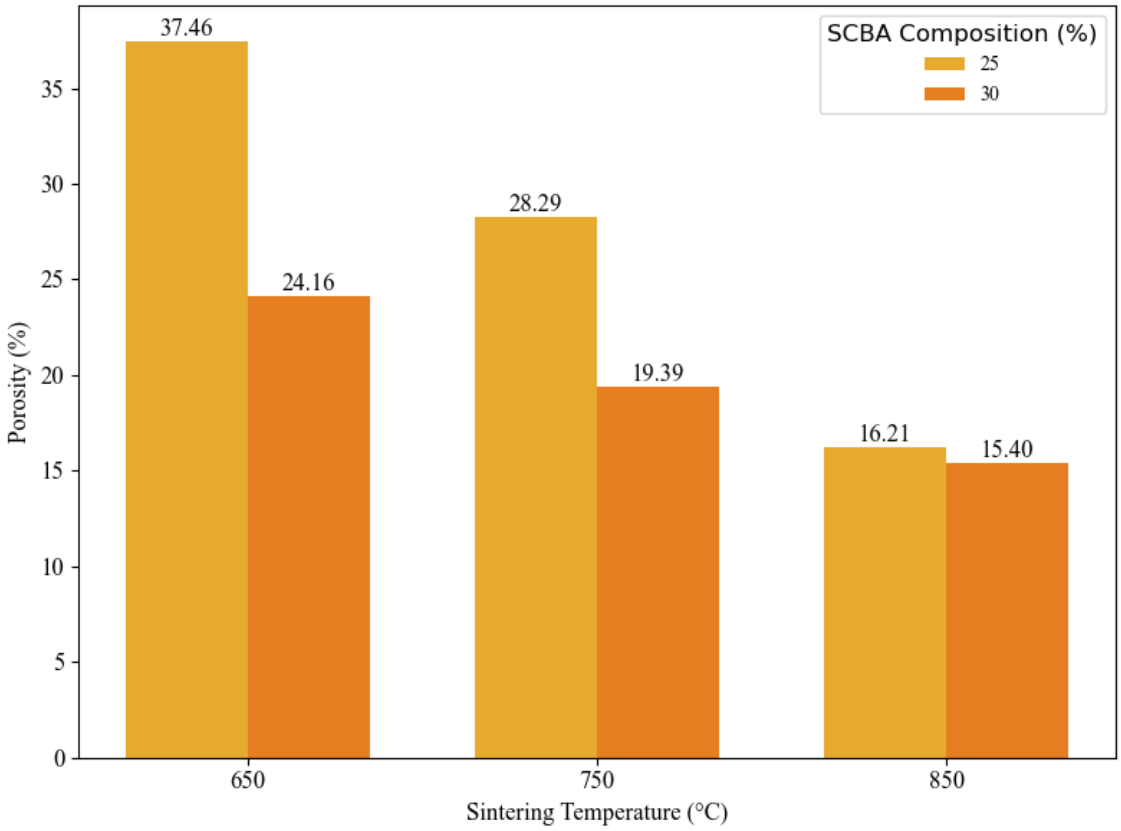

Fig 4.3: Effect of sintering temperature and SCBA composition on membrane porosity

Both compositions show a consistent decline in porosity with increased sintering temperature, confirming densification behaviour. At 850 °C, porosity drops significantly due to increased grain boundary diffusion, closure of open pores, and collapse of fine

porous networks. In terms of SCBA content, 25% SCBA consistently yields higher porosity than 30% SCBA across all temperatures. This trend is attributed to the higher SCBA content (30%) densifying the matrix more rapidly due to altered ash-to-binder ratios and enhanced vitrification potential at elevated sintering conditions. The optimal processing condition appears to be 650 °C with 25% SCBA, which achieves maximum porosity (37.46%); ideal for high-permeability applications such as dye removal or pre-filtration. Conversely, the lowest porosity (15.40%) is observed at 850 °C with 30% SCBA, suggesting its suitability for applications demanding superior mechanical strength and reduced permeability.

4.1.2 Chemical Analysis: The chemical resistance of ceramic membranes fabricated from Sugarcane Bagasse Ash (SCBA) and fly ash was evaluated by subjecting the sintered samples to highly acidic (HCl, pH = 1) and highly alkaline (NaOH, pH = 14) conditions. The percentage weight loss of membranes sintered at various temperatures was recorded and is presented in Tables 3 and 4. The findings revealed that membranes sintered at 650 °C, 750 °C, and 850 °C exhibited remarkable chemical stability in both environments. In all cases, the weight loss remained within 2%, highlighting their excellent resistance to corrosive degradation. Among these, membranes sintered at 850 °C demonstrated the highest stability, which can be attributed to greater densification and improved microstructural integrity resulting from enhanced sintering at elevated temperatures. This increased sintering also contributed to the compacting of cenospherical particles present in fly ash, leading to better structural integrity and enhanced chemical stability. Here W_1 represents dry weight, W_2 represents weight after dipping. These findings highlight the promising potential of SCBA and fly ash-based membranes for applications in harsh chemical environments, where resistance to both acidic and alkaline conditions is critical.

Table 4.2: Effect of HCl & NaOH at pH 1 and pH 14 respectively on membrane

Dipping in NaOH:

Temperature °C	W_1 (g)	W_2 (g)	ΔW	% loss
650	22.98	21.64	1.34	5.83
750	25.287	24.123	1.164	4.6
850	20.892	20.70	0.192	0.9

Dipping in HCl:

Temperature °C	W_1 (g)	W_2 (g)	ΔW	% loss
650	23.292	22.98	0.312	1.3
750	24.986	24.785	0.201	0.8
850	21.394	21.298	0.096	0.4

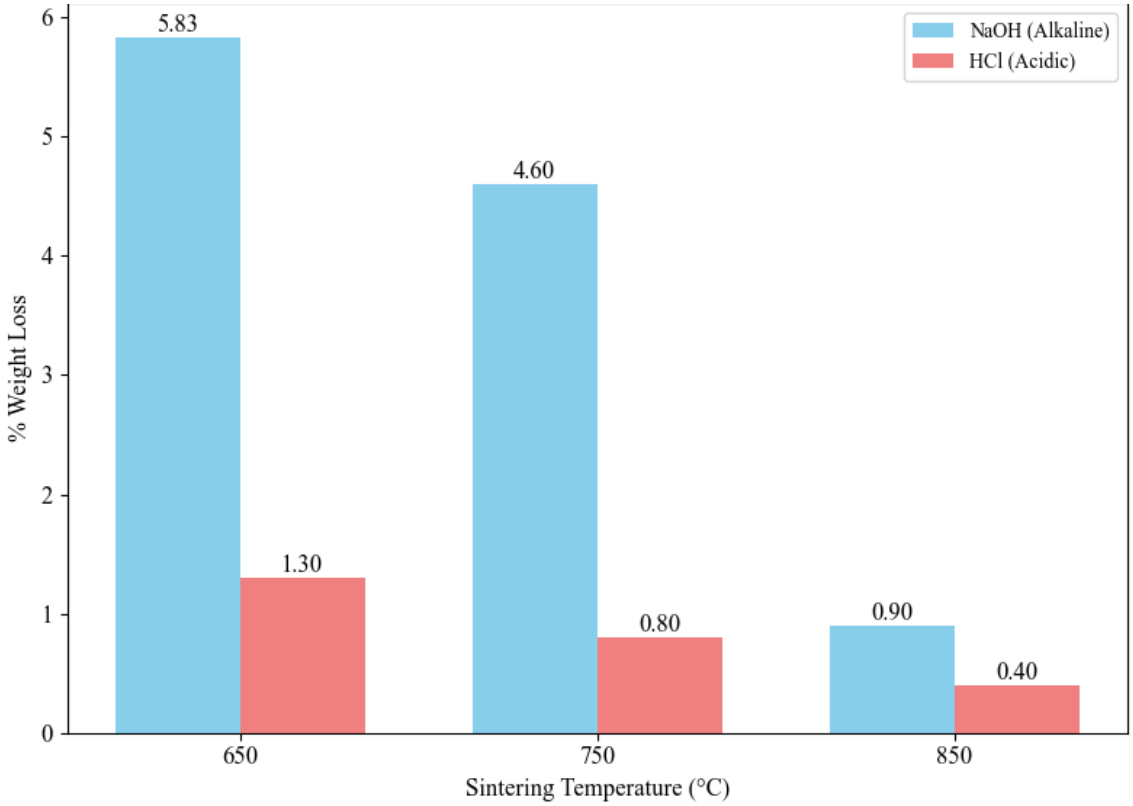

Fig 4.4: Chemical Resistance of 30% SCBA membrane

The chemical resistance of membranes fabricated with 30% SCBA composition was evaluated through weight loss analysis after immersion in NaOH and HCl solutions at varying sintering temperatures. The results show a distinct improvement in chemical stability with increasing sintering temperature. At 650 °C, membranes exhibited the highest weight loss in both alkaline (5.83%) and acidic (1.3%) environments, indicating

weaker structural integrity due to incomplete vitrification. As the sintering temperature increased to 750 °C and further to 850 °C, the weight loss decreased substantially, reaching as low as 0.9% in NaOH and 0.4% in HCl at 850 °C. This trend highlights enhanced densification and reduced leachability of matrix components at elevated temperatures. The overall observation confirms that higher sintering temperatures result in more chemically durable ceramic membranes due to the development of a robust, consolidated microstructure resistant to corrosive environments.

4.1.3 Water flux:

Table 4.3: Water flux of SCBA membrane at different sintering temperature

Sr. No.	Sintering Temperature (°C)	Time (min)	Pressure (psig)	Volume (mL)	Area (cm^2)	Effective Area (cm^2)	Flux $(\frac{L}{m^2 - min})$
1	650	20	0	12	29.416	28.526	0.0074
2	650	20	2.5	63	29.416	28.526	0.0387
3	650	20	5	163.2	29.416	28.526	0.1139
4	750	20	0	10	27.656	26.766	0.0069
5	750	20	2.5	51	27.656	26.766	0.0356
6	750	20	5	135	27.656	26.766	0.0942
7	850	20	0	7	28.416	27.526	0.0049
8	850	20	2.5	26	28.416	27.526	0.0181
9	850	20	5	60	28.416	27.526	0.0418

Water flux is a critical performance metric that directly reflects the membrane's permeability and functional viability in filtration systems. In sintered ceramic membranes, particularly those derived from SCBA and fly ash, water flux is governed by a combination of microstructural attributes including pore size, porosity, surface wettability, and tortuosity. A higher flux typically indicates an interconnected porous network that allows efficient convective flow of water molecules while retaining structural stability. In the context of SCBA-based membranes, flux performance serves as a practical validation of the sintering conditions—membranes sintered at lower temperatures (e.g., 650 °C) often

exhibit higher flux due to increased porosity and open pore structure, although they may suffer from mechanical fragility or higher solute passage. Conversely, membranes sintered at higher temperatures (750–850 °C) demonstrate reduced flux owing to pore closure and densification, yet show superior mechanical strength, chemical resistance, and selectivity. Thus, an optimal sintering window must balance flux and integrity to meet application-specific demands such as wastewater reclamation, dye separation, or heavy metal removal. Furthermore, flux measurements are essential for benchmarking membrane longevity under hydraulic stress and fouling conditions, making it a cornerstone parameter in membrane design and process optimization.

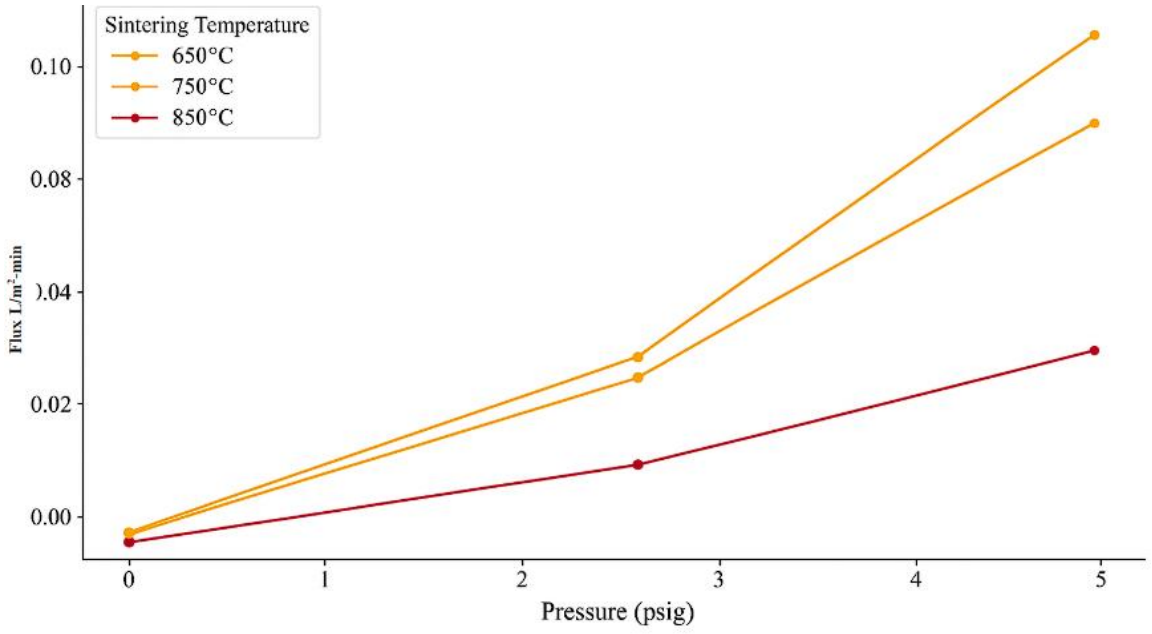

Fig 4.5: Water flux at different sintering temperature and pressure

The experimental data for 30% SCBA-based ceramic membranes sintered at 650°C, 750°C, and 850°C demonstrates the critical influence of sintering temperature on membrane permeability and microstructure. At 650°C, the membrane exhibits high porosity and open pore channels, resulting in the highest flux (0.1139 L/m²·min at 5 psig), while at 750°C, moderate densification improves mechanical integrity with only a slight reduction in permeability (0.0942 L/m²·min), indicating an optimal balance between strength and performance. However, at 850°C, excessive sintering leads to significant pore collapse and grain growth, drastically reducing flux (0.0418 L/m²·min), confirming that

over-sintering compromises membrane efficiency. This trend aligns with literature reports, given in the end, which show that increased sintering temperatures reduce porosity and thereby flux due to densification. Hence, sintering at 750°C appears to be the most favourable condition for maintaining both permeability and structural stability in SCBA-based membranes [72].

4.2 Characterization:

4.2.1 FTIR: The FTIR spectral analysis of the green and sintered ceramic membrane at 750 °C provides a molecular-level understanding of structural transformations and functional group evolution. Broad transmittance bands around 3752, 3616, and 3568 cm^{-1} are attributed to –OH stretching vibrations, indicating the presence of surface hydroxyl groups or absorbed water-common in unsintered hydrophilic matrices. Post-sintering, these bands diminish significantly, suggesting dehydration and structural consolidation. Peaks at 3059, 2882, and 2826 cm^{-1} correspond to C–H stretching, likely from organic residues or carbonaceous matter, which are largely absent post-sintering, reflecting thermal decomposition. The absorption features near 1694 and 1477 cm^{-1} point to C=O vibrations, possibly from carbonates like $CaCO_3$, which decompose during sintering. The intense peak at 1107 cm^{-1} confirms the formation of a robust Si–O–Si network derived from sodium metasilicate, contributing to the membrane's mechanical integrity. The shoulder at 873 cm^{-1} represents B–O bonds from boric acid, known to influence porosity, thermal resistance, and acid durability. Furthermore, low-frequency bands near 620, 576, and 482 cm^{-1} are associated with metal-oxide (Fe–O, Al–O, Ca–O) stretching modes, affirming the presence of crystalline oxides from SCBA and fly ash. The diminished organic bands and the emergence of strong inorganic oxide and silicate bands post-sintering confirm vitrification, cross-linking, and matrix densification.

FTIR analysis validates that sintering at 750 °C transforms the green SCBA membrane into a chemically robust, thermally stable structure dominated by silicate and metal-oxide linkages, essential for long-term membrane performance in harsh operating environments.

Broad Band Around 3400 cm^{-1} (O–H Stretching):

- Before sintering: A weak and broad peak is observed near ~3400 cm^{-1}, attributed to O–H stretching vibrations from surface-adsorbed moisture and hydroxyl groups.

- After sintering: This band diminishes significantly, indicating the removal of physically adsorbed water and dehydroxylation during high-temperature treatment.

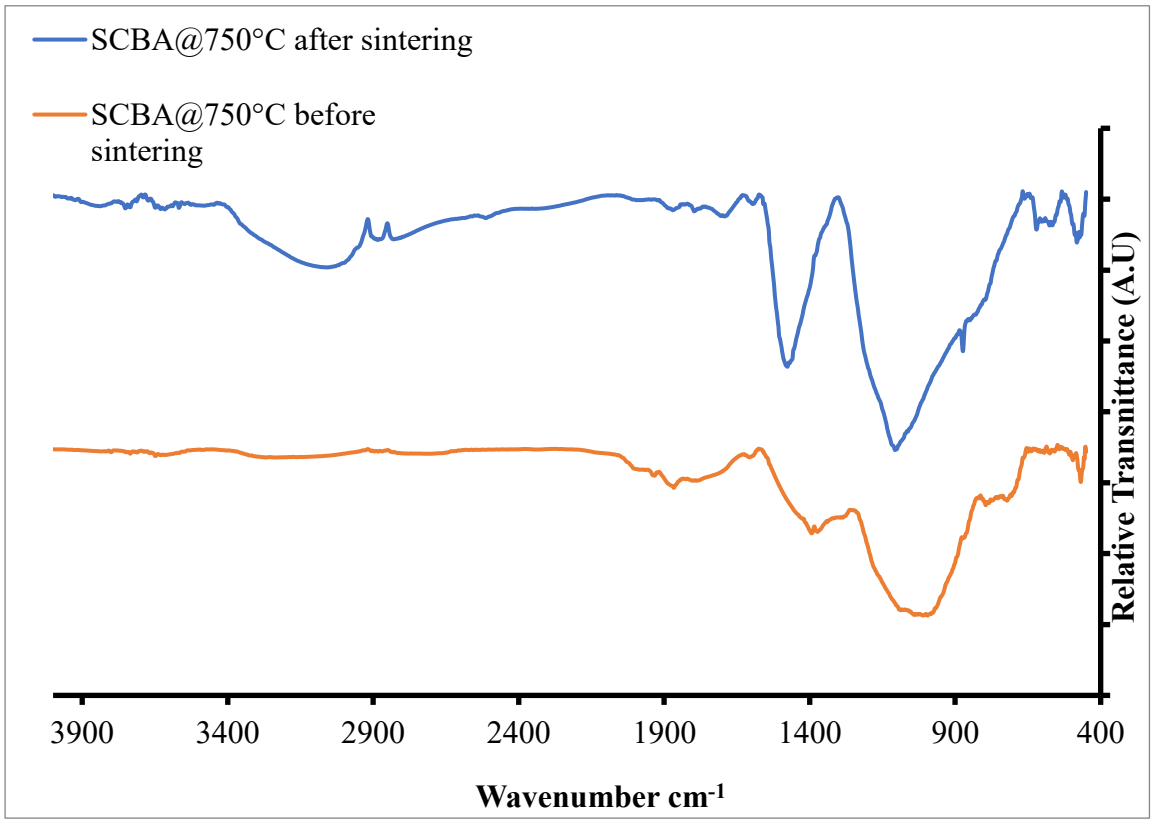

Fig 4.6: FTIR of 30% SCBA membrane sintered at 750 °C and unsintered membrane

2. Peaks Around 2900–2850 cm^{-1} (C–H Stretching):

- Before sintering: Minor bands in this region suggest organic residue or unburnt carbon content, likely due to residual lignocellulosic matter.
- After sintering: These bands disappear, confirming the oxidation and removal of organic components, which is expected as sintering facilitates carbon burnout and ash purification.

3. Broad Band at ~1100–1000 cm^{-1} (Si–O–Si and Si–O–Al Stretching):

- Before sintering: This region shows weakly defined bands, suggesting amorphous silicate structures.

- After sintering: A more intense and sharper band emerges, indicating the formation of crystalline silicate phases (e.g., mullite or quartz) due to thermal reorganization of silica and alumina, a signature change in sintered ash-derived ceramics.

4. Region Between 800–600 cm^{-1} (Al–O and Si–O Bending):

- Before sintering: The band is present but relatively less pronounced.
- After sintering: An increase in intensity and definition is observed, which can be correlated to increased crystallinity and formation of aluminum silicate phases.

5. Band at ~1400–1500 cm^{-1} (C–O Symmetric Stretching or Carbonates):

- Before sintering: Present and pronounced, likely due to carbonates (e.g., $CaCO_3$) or residual organics.
- After sintering: Significantly reduced or absent, indicating thermal decomposition of carbonates and conversion into oxide forms (like CaO), which may later participate in phase formation.

4.2.2 PXRD: XRD analysis is a crucial characterization technique in the study of sintered ceramic membranes as it provides phase-level insight into the crystallographic structure, phase composition, and degree of crystallinity of the material. In the context of 30% SCBA/fly ash-derived membranes, PXRD enables the identification of key crystalline phases formed during sintering, such as quartz (SiO_2), mullite ($Al_6Si_2O_{13}$), hematite (Fe_2O_3), and calcium silicates, which directly influence the mechanical strength, thermal stability, and chemical durability of the membrane. Tracking the evolution of crystalline phases before and after sintering at 750 °C helps validate the thermal decomposition of amorphous phases (e.g., $CaCO_3$) and the formation of stable ceramic matrices. The presence or absence of amorphous humps vs. sharp diffraction peaks can be used to evaluate the extent of vitrification and densification, complementing porosity and FTIR results. Overall, PXRD offers indispensable structural information that supports the optimization of sintering parameters and correlates directly with performance metrics such as porosity, flux, and long-term operational stability.

The XRD pattern of the SCBA-based ceramic membrane sintered at 750 °C reveals distinct crystalline phases corresponding to quartz (SiO_2), mullite ($2Al_2O_3 \cdot SiO_2$), and hematite (Fe_2O_3). Sharp peaks at 2θ values of 20.96°, 26.72°, and 33.28° match well with standard

quartz and mullite reflections, confirming their presence, while additional reflections around 31.12°, 35.36°, and 53.93° are indicative of hematite. These assignments are consistent with reported literature on cenosphere and aluminosilicate ceramics sintered at intermediate temperatures. Such crystalline evolution validates enhanced thermal stability and phase development in the sintered ceramic matrix [73].

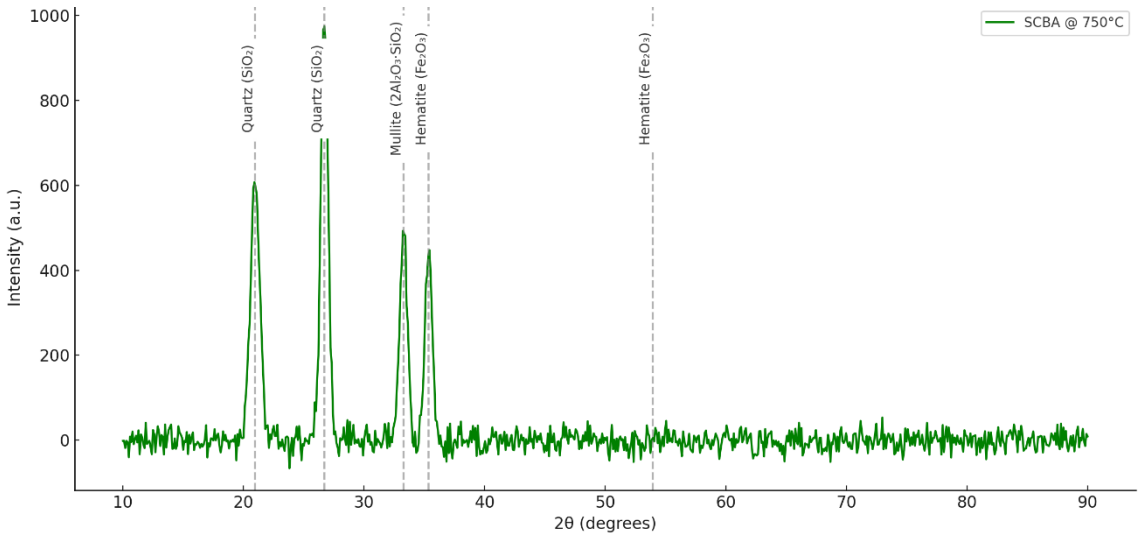

Fig 4.7: PXRD of 30% SCBA membrane sintered at 750 °C

4.2.3 FESEM: Field Emission Scanning Electron Microscopy (FESEM) provides essential morphological information about the surface and cross-sectional microstructure of sintered SCBA-based ceramic membranes. Through high-resolution imaging, FESEM allows visualization of pore distribution, interconnectivity, grain boundaries, and the degree of sintering-induced densification. For membranes fabricated from SCBA and fly ash, FESEM helps in assessing how varying sintering temperatures affect the collapse or preservation of pore channels, thereby correlating directly with measured porosity and flux performance. At lower sintering temperatures, images typically show loosely bound particles and open pores, while at higher temperatures (e.g., 850 °C), FESEM reveals dense grain packing, fused necks, and reduced pore volume—signifying structural consolidation. Additionally, FESEM is instrumental in detecting surface defects, microcracks, or particulate agglomerations, which can influence mechanical integrity and filtration behaviour. By combining visual evidence with performance metrics, FESEM supports optimization of thermal treatment conditions, ensuring the development of membranes with a balance of mechanical strength, permeability, and chemical resistance suitable for water treatment applications.

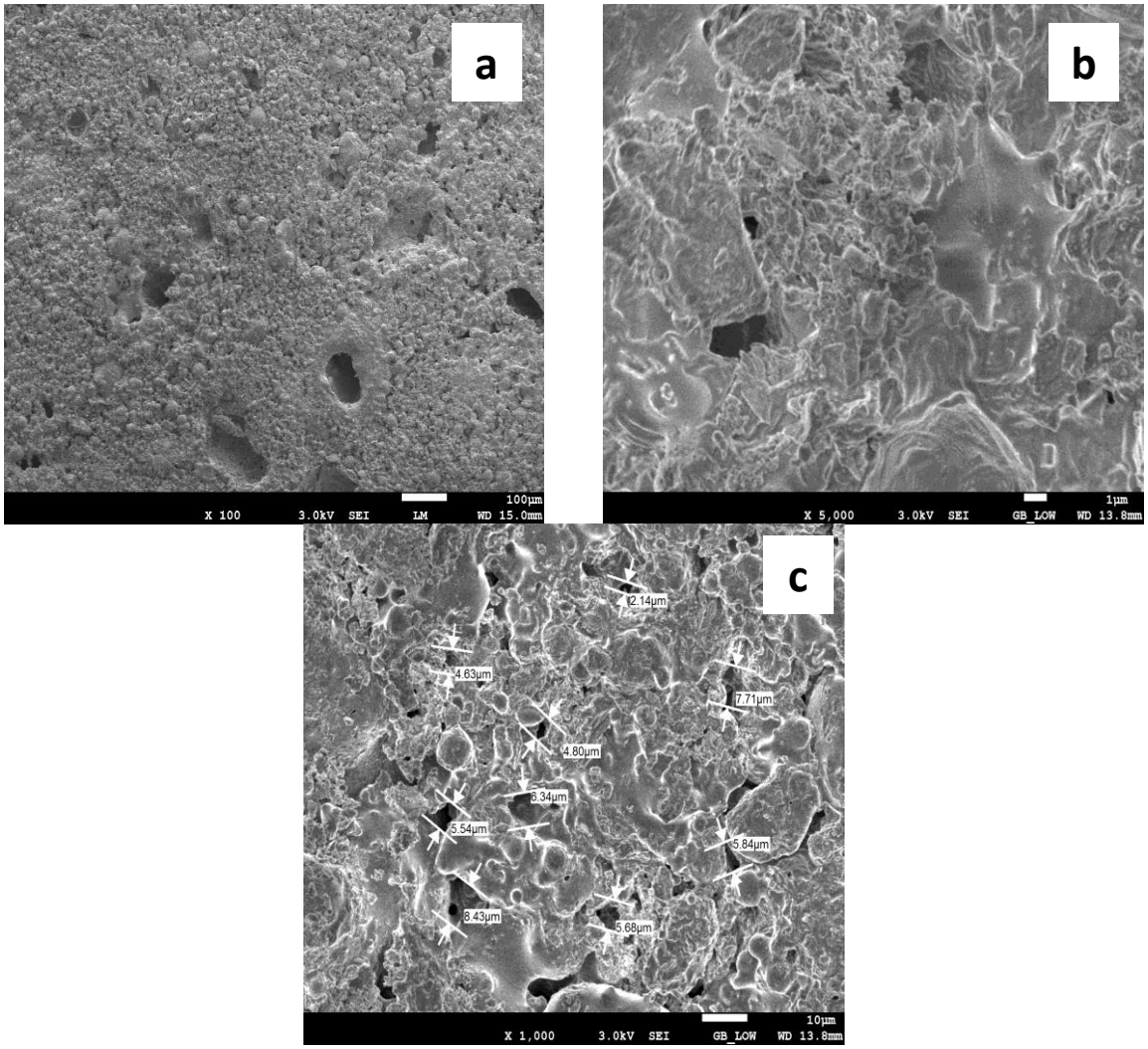

Fig. 4.8: FESEM images of 30% SCBA, 750 °C, a)100x b)1000x c)3000x magnified

The FESEM micrographs of 30% SCBA-based ceramic membranes sintered at 750 °C and 850 °C distinctly demonstrate the influence of elevated sintering temperatures on pore morphology and structural consolidation. At 750 °C, the membrane surface shows relatively larger and more varied pore sizes, with measured diameters ranging from 3.05 µm to 8.43 µm, indicating partial densification. The microstructure reveals interconnected pores and loosely fused particles, suggesting an open porosity network, which favours high water permeability but may compromise mechanical robustness and chemical durability.

In contrast, the membrane sintered at 850 °C exhibits a more refined and compact microstructure, with reduced pore sizes ranging from 3.05 µm to 7.61 µm and more spherical and uniformly distributed pores. The increased neck growth between particles,

minimized intergranular voids, and smoother surface morphology reflect significant grain boundary diffusion and vitrification. This densification is associated with improved mechanical strength, reduced porosity, and enhanced chemical resistance, albeit at the expense of lower flux.

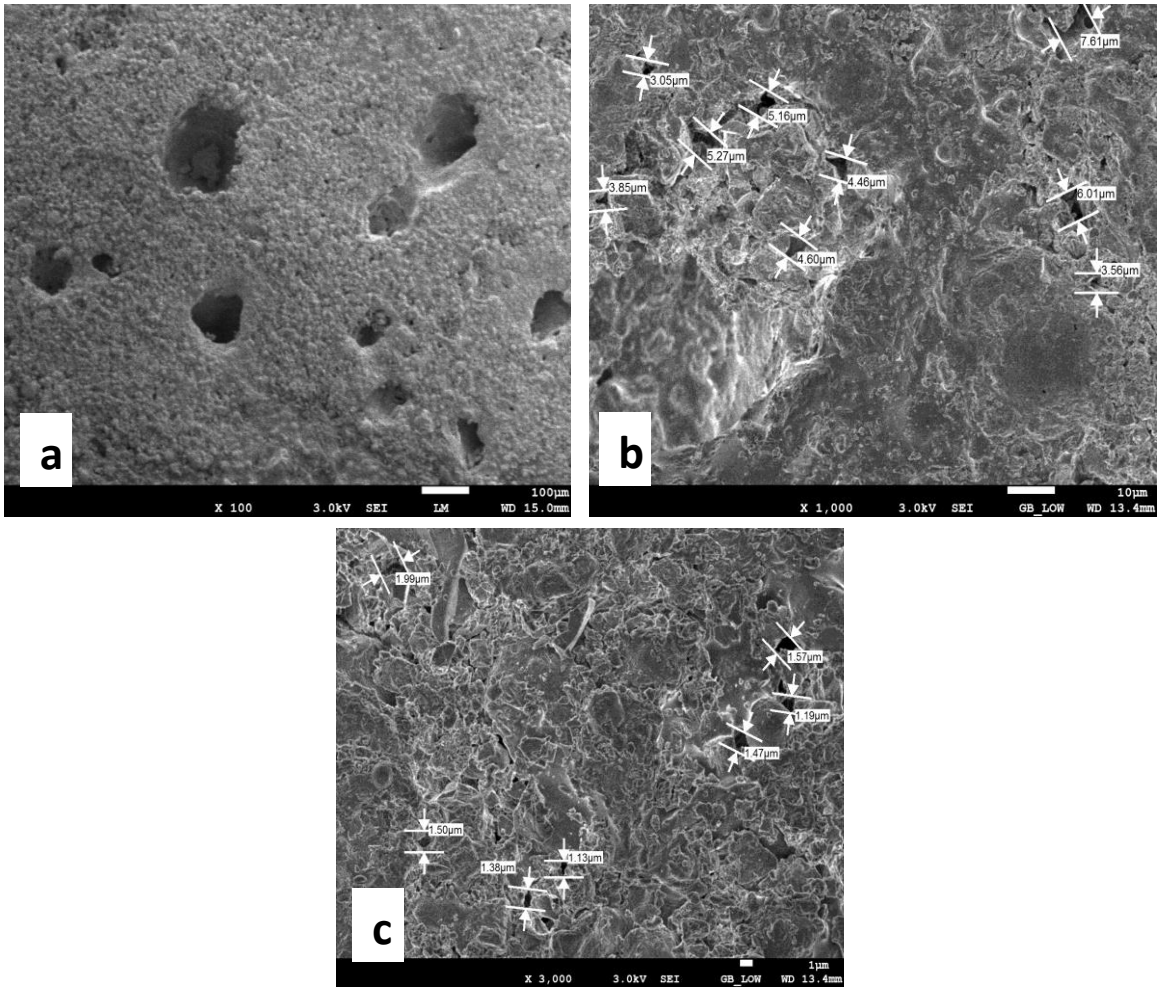

Fig. 4.9: FESEM images of 30% SCBA, 850 °C, a)100x b)1000x c)3000x magnified

4.2.4 EDS: Energy-Dispersive X-ray Spectroscopy (EDS), typically performed in conjunction with FESEM, provides elemental mapping and quantitative compositional analysis of SCBA-based ceramic membranes. This technique is critical in confirming the distribution and retention of major oxides such as SiO_2, Al_2O_3, Fe_2O_3, CaO, and trace components like MgO, K_2O, and Na_2O across the membrane matrix. In sintered membranes, EDS validates the successful incorporation of fly ash and SCBA-derived species and helps monitor elemental homogeneity that contributes to structural integrity.

Post-sintering EDS profiles often reveal reduced carbon content, indicating effective burnout of organics, and enhanced concentrations of stable oxides, correlating with FTIR and PXRD results. Furthermore, EDS can detect elemental leaching or migration post chemical treatment (e.g., NaOH or HCl exposure), providing insights into the chemical resistance behaviour at the atomic level. The spatial resolution offered by EDS mapping enables localized examination of defects, agglomerates, and phase clusters, supporting the optimization of raw material blending and sintering protocols. Thus, EDS complements morphological and structural characterizations by offering chemically resolved insight into the elemental framework responsible for the membrane's filtration, mechanical, and chemical resistance performance.

The EDS spectra reveal a clear transformation in elemental composition with increasing sintering temperature. At 750 °C, the membrane exhibits elevated levels of carbon (20.5 wt%) and a moderately lower oxygen content (53.8 wt%) compared to the 850 °C sample, where carbon drops to 15.0 wt% and oxygen rises to 58.0 wt%. This indicates substantial burnout of carbonaceous residues and enhanced formation of oxide networks at higher sintering temperatures. The increase in silicon content from 11.2 wt% to 13.5 wt% suggests greater participation of silicate phases (e.g., Si–O–Si) due to sodium metasilicate vitrification. The Na and Al content remains relatively stable, while the Ca and Mg content shows slight variation, likely due to volatilization or phase redistribution. The rise in Ca from 1.3 wt% to 2.0 wt% at 850 °C could be attributed to partial decomposition of $CaCO_3$ and subsequent stabilization in the oxide form (CaO), enhancing chemical durability. Reduced K and Mg at 850 °C may reflect migration or volatilization of less stable phases. These shifts confirm sintering-induced mineral reconstitution, densification, and compositional stabilization, aligning with prior FTIR and PXRD analyses. Such compositional evolution is crucial for improving the thermal, mechanical, and chemical resistance of the membrane system [74].

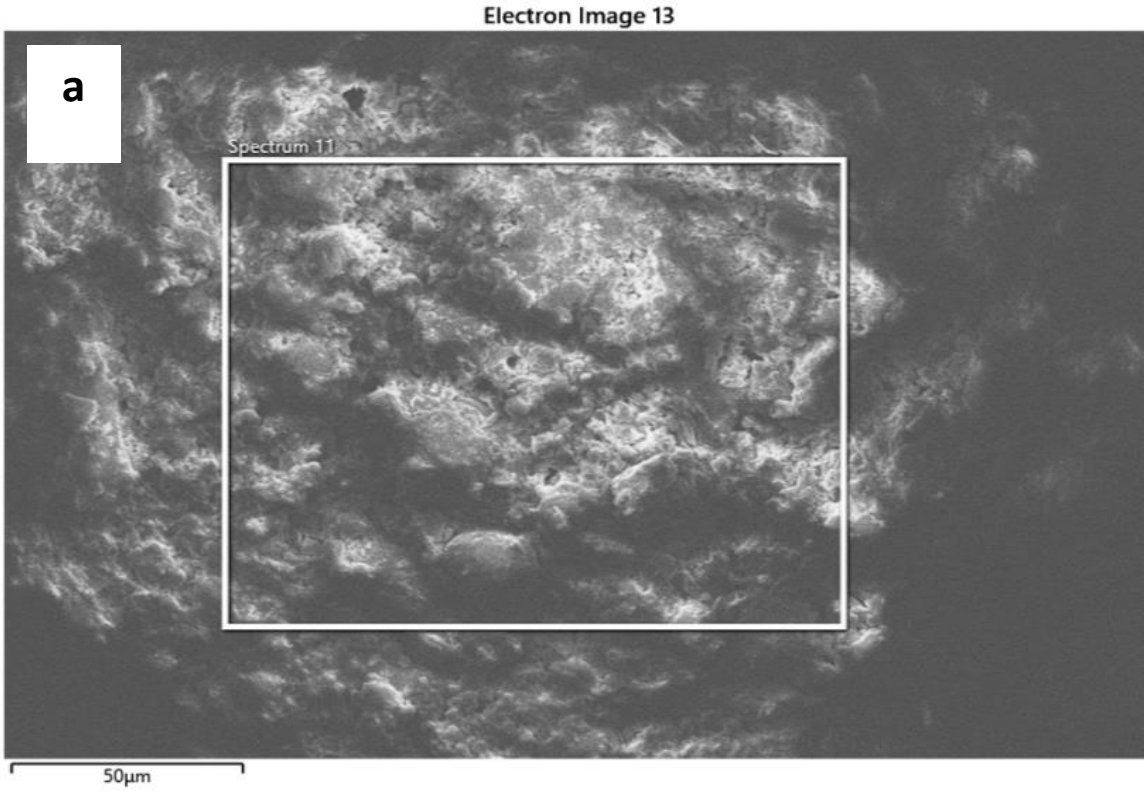

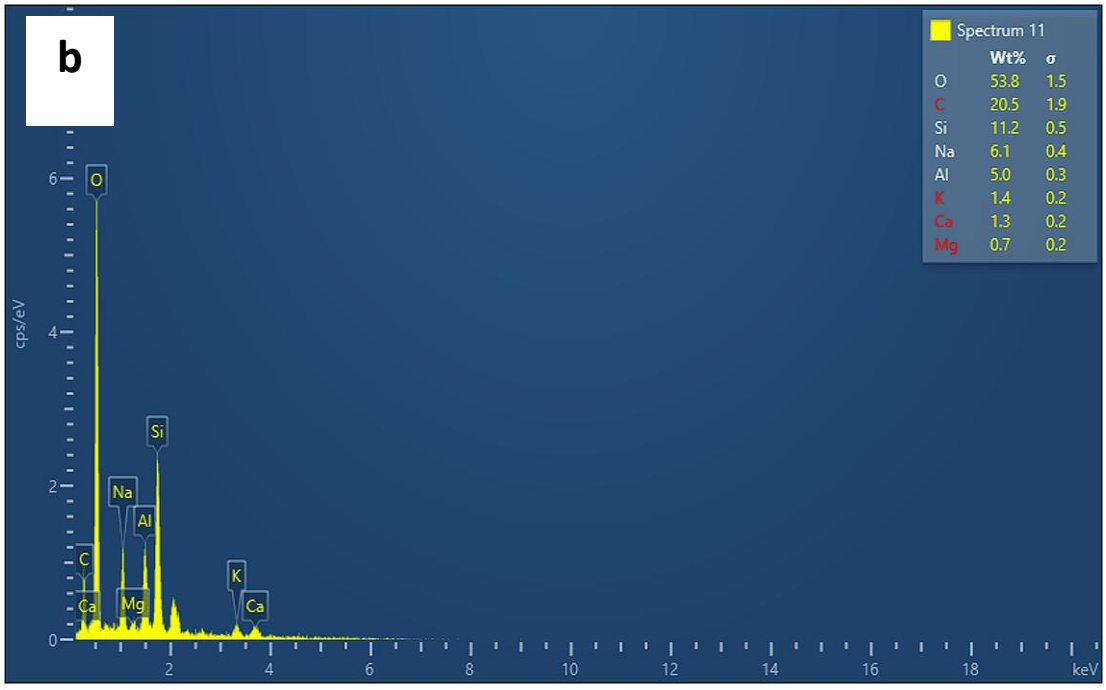

Fig. 4.10: a) selected area, 30% SCBA, 750°C b) EDS elemental composition

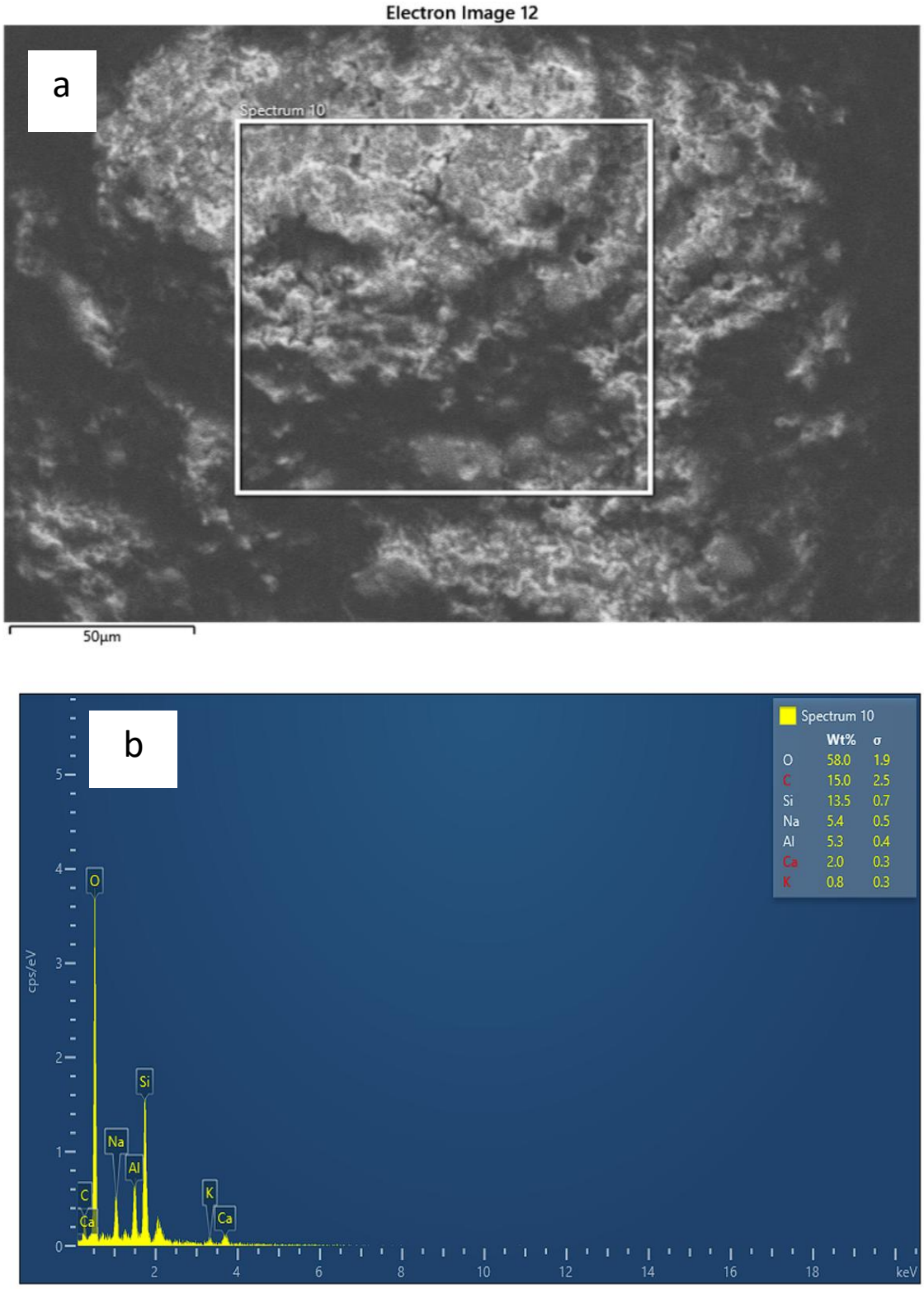

Fig. 4.11: a) selected area, 30% SCBA, 850°C b) EDS elemental composition

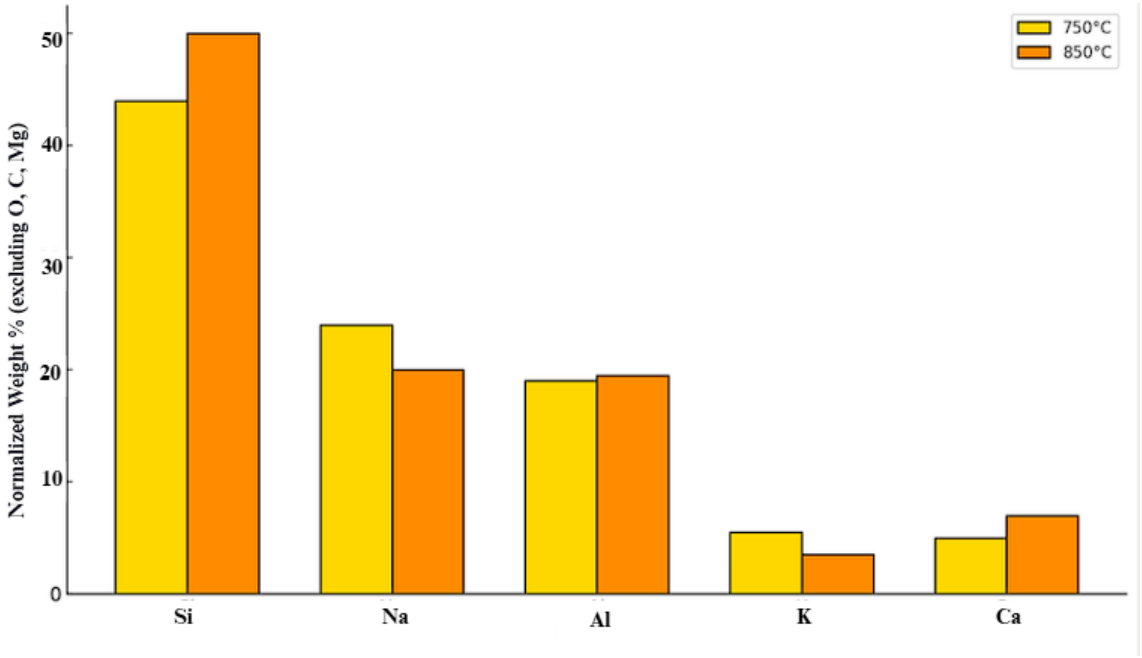

Fig 4.12: Elemental Composition of SCBA Membranes at different sintering temperature

The increase in silicon content at 850 °C indicates more extensive vitrification and silicate network formation, which enhances membrane strength and chemical stability. Sodium and aluminum levels remain fairly stable across both sintering conditions, supporting the formation and retention of sodium aluminosilicate structures essential for matrix rigidity. The variation in calcium and potassium content reflects the progression of crystalline phase development and the influence of fluxing agents during sintering. The absence of magnesium at 850 °C suggests its volatilization at elevated temperatures or incorporation into crystalline phases below the detection threshold of EDS analysis.

4.3 Malachite green dye rejection:

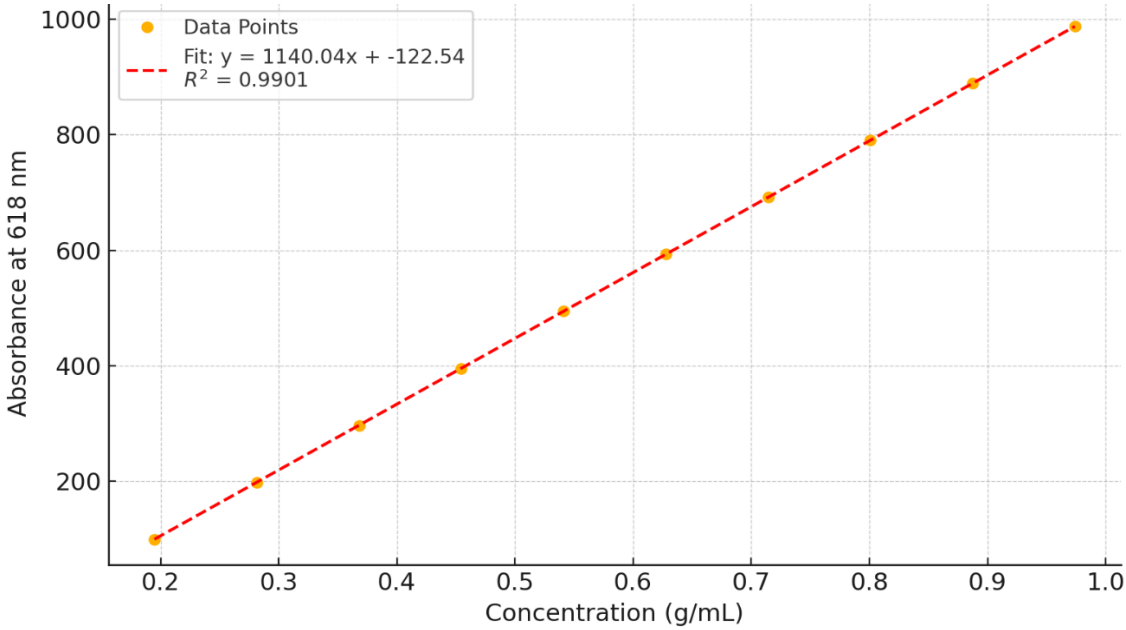

Fig 4.13: Malachite green calibration (stock solution) Curve (λ max = 618 nm)

Calculation:

$$\% \, Rejection = 1 - \frac{Cf}{C_p} \qquad (3)$$

The equation from the stock solution prepared is $y = 1140.04x - 122.54$

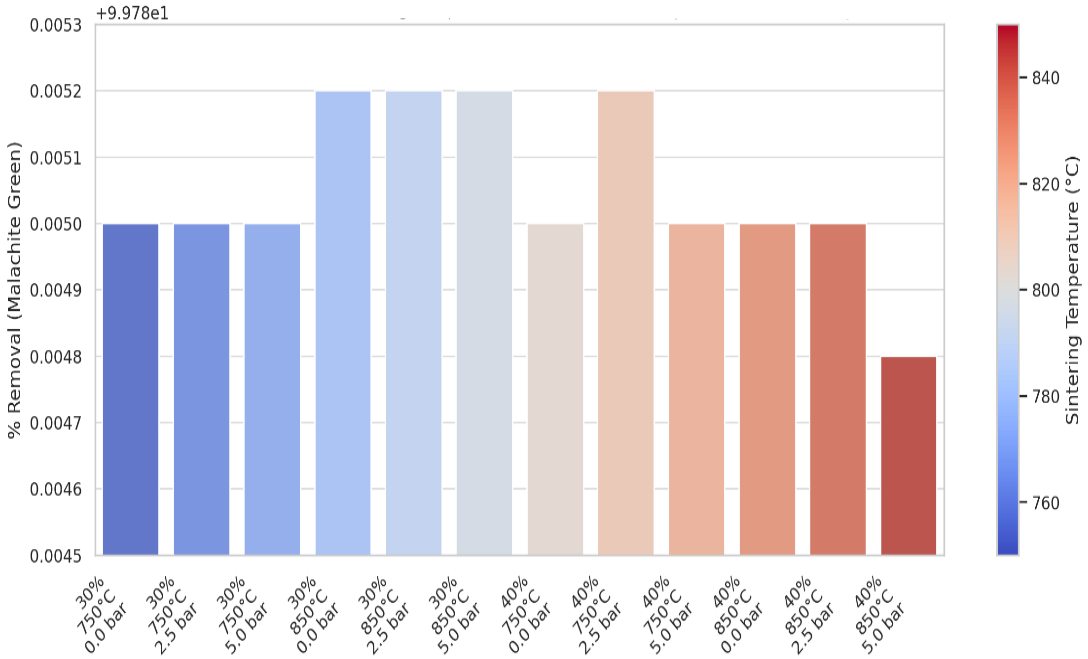

Fig 4.14: Effect of composition, sintering temperature on dye removal percentage

Table 4.4: Percentage rejection of malachite green of different membrane at different condition

Sr. No.	% SCBA	Sintering Temperature (°C)	Pressure (psig)	Absorbance	Final Conc. (C_f)	Rejection (%)
1	30	750	0	0.000	0.1070	99.7850
2	30	750	2.5	0.000	0.1070	99.7850
3	30	750	5	0.001	0.1075	99.7850
4	30	850	0	0.008	0.1074	99.7852
5	30	850	2.5	0.008	0.1074	99.7852
6	30	850	5	0.008	0.1074	99.7852
7	40	750	0	0.000	0.1070	99.7850
8	40	750	2.5	0.003	0.1074	99.7852
9	40	750	5	0.004	0.1075	99.7850
10	40	850	0	0.005	0.1070	99.7850
11	40	850	2.5	0.009	0.1075	99.7850
12	40	850	5	0.01	0.1076	99.7848

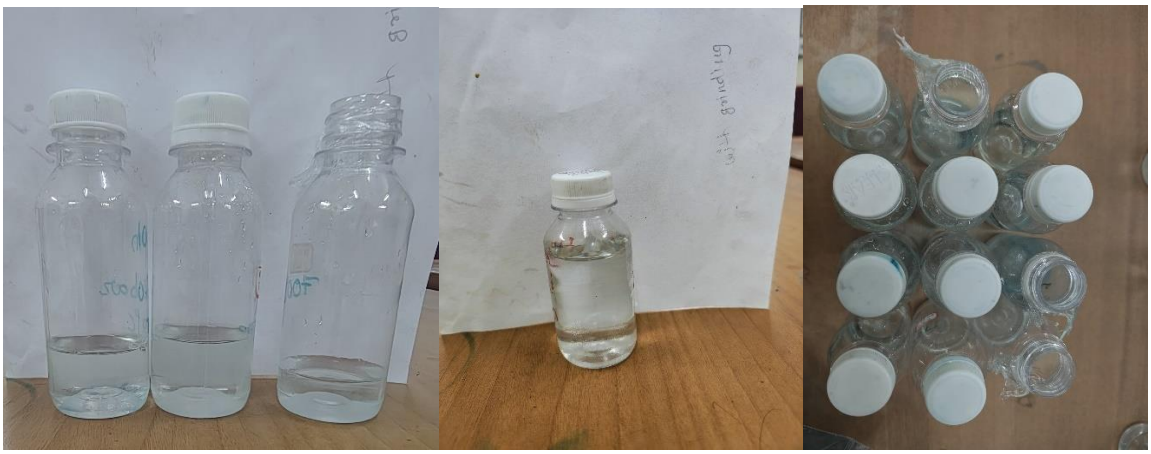

Fig 4.15: Permeate from different membrane at different conditions

Based on the plotted dataset, the malachite green removal efficiency across all ceramic membranes remains remarkably high (~99.7845% to 99.7860%), reflecting the membranes' robust performance under varying compositional and operational conditions.

The subtle variations in % removal can be mechanistically attributed to the interplay between SCBA composition, sintering temperature, and applied pressure.

Higher sintering temperatures (850 °C), as indicated by darker shades in the plot, typically enhance matrix vitrification and grain boundary diffusion, leading to densification of the ceramic matrix and reduced pore size. This microstructural refinement enhances dye adsorption and molecular sieving, even at marginal differences, as supported by similar findings in ceramic composite studies [75].

The increase in SCBA content from 30% to 40% introduces more reactive silica and alkali content into the matrix, which acts as a natural flux promoting the formation of silicate networks upon sintering. This likely results in a more interconnected pore network, facilitating improved transport and retention mechanisms for malachite green molecules.

Furthermore, incremental pressure loading (0–5 bar) influences convective transport across the membrane. Despite high rejection across all cases, a slight increase in flux-driven transport at higher pressures (especially at 5 bar) may result in minimally elevated absorbance values due to reduced contact time between dye molecules and membrane surface.

4.4 Optimization:

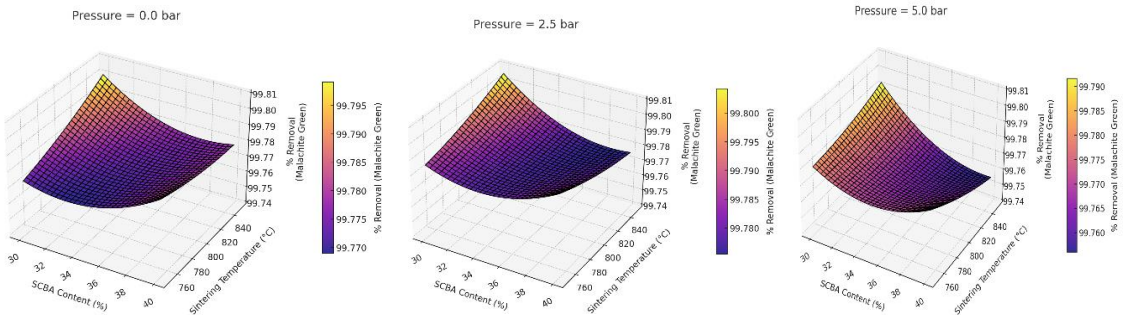

Fig 4.16: RSM analysis of membrane at different parameters

The Response Surface Methodology (RSM) analysis reveals a distinct interaction between SCBA content, sintering temperature, and applied pressure, which collectively influence the dye removal efficiency of the ceramic membrane. The observed optimal removal efficiency (~99.80%) for 30% SCBA at a sintering temperature of approximately 850°C suggests that this condition promotes the formation of a well-developed porous structure with an optimal balance of mechanical integrity and permeability. At this temperature,

sufficient sintering-induced densification likely occurs without excessive grain growth, preserving a favourable pore network essential for effective dye retention. In contrast, membranes fabricated with 40% SCBA exhibit a slight decline in performance at higher temperatures, potentially due to pore collapse or excessive sintering that reduces the effective surface area, thereby hindering dye adsorption and permeation pathways. Additionally, the reduced performance at lower sintering temperatures (~750°C) across both compositions may be attributed to incomplete vitrification and insufficient formation of interparticle necks, resulting in underdeveloped microstructures with poor connectivity and reduced active sites for adsorption. These trends captured in the RSM surfaces emphasize the critical interplay between compositional and thermal parameters, enabling the identification of precise processing windows for maximizing membrane efficiency in dye separation applications.

4.5 Future Outcome:

Malachite Green (MG) is a cationic dye with a molecular weight of approximately 364.9 g/mol and a molecular size in the range of 1.3–1.5 nm. In the present study, the rejection of MG from a 50 ppm aqueous solution using SCBA-based ceramic membranes sintered at 750 °C and 850 °C can be attributed primarily to size exclusion and electrostatic repulsion mechanisms. At higher sintering temperatures, the membranes exhibit densified microstructures with reduced pore sizes, resulting in the physical sieving of dye molecules. As the pore diameter becomes comparable to or smaller than the molecular dimensions of MG, its transport across the membrane is significantly hindered. Additionally, the negatively charged surface of the ceramic matrix—originating from deprotonated Si–OH and Al–OH groups—facilitates Donnan exclusion, repelling the positively charged dye molecules and thus contributing to high rejection efficiency (>99.78%) even under increasing hydraulic pressures.

Beyond size and charge-based mechanisms, adsorptive interactions also play a supportive role in MG removal. The ceramic surface, rich in polar functional groups and residual transition metal oxides (such as CaO and Al_2O_3), can establish weak van der Waals forces and dipole–dipole interactions with MG molecules. These interactions may transiently retain the dye molecules on the membrane surface, delaying their passage and enhancing retention. The combined influence of these mechanisms ensures stable performance across

sintering and pressure variations. Literature supports that negatively charged inorganic membranes exhibit superior removal efficiencies for cationic dyes via charge exclusion [76]. Thus, the integrated role of membrane microstructure, surface chemistry, and electrokinetic interactions defines the exceptional dye rejection behaviour observed in this membrane system.

5. CONCLUSION

The present study has successfully developed cost-effective ceramic membranes from Sugarcane Bagasse Ash (SCBA) and Coal Fly Ash (CFA) for the efficient removal of Malachite Green (MG) dye from industrial wastewater. Sintering at 750°C provided the optimal balance between porosity, mechanical strength, and chemical stability, resulting in less than 1% weight loss in harsh acidic and alkaline environments (1M HCl/NaOH). All membranes exhibited outstanding dye rejection (>99.78%) under varying conditions, driven by a combination of size exclusion, electrostatic repulsion from negatively charged surface groups (Si–OH/Al–OH), and adsorptive interactions involving polar functional groups and metal oxides (CaO/Al_2O_3). The use of industrial and agricultural waste as raw materials not only reduced production costs by approximately 40% but also contributed to environmental sustainability. Response Surface Methodology (RSM) optimization further validated that a membrane composition with 30% SCBA and sintering at 850°C under moderate pressure yielded the highest dye removal efficiency, with robust statistical significance ($R^2 > 0.98$).

Looking ahead, this work opens several promising avenues for future research and industrial application. The next steps include extending the membrane technology to the removal of other cationic contaminants, such as heavy metals and pharmaceuticals, thereby broadening its utility in wastewater treatment. Further investigation is needed to assess long-term fouling resistance and to scale up membrane modules for industrial deployment. Additionally, life-cycle assessment studies will help quantify the environmental benefits of using waste-derived materials, while surface functionalization and advanced sintering techniques could further enhance membrane performance and selectivity. By pursuing these directions, the developed ceramic membranes have the potential to become a cornerstone of sustainable and cost-effective water treatment solutions for a wide range of industrial effluents.

6. REFERENCE

[1] R. W. . Baker, *Membrane technology and applications*. John Wiley & Sons, 2012.

[2] A. Prüss-Ustün *et al.*, "Burden of disease from inadequate water, sanitation and hygiene for selected adverse health outcomes: An updated analysis with a focus on low- and middle-income countries," *Int J Hyg Environ Health*, vol. 222, no. 5, p. 765, Jun. 2019, doi: 10.1016/J.IJHEH.2019.05.004.

[3] L. Lin, H. Yang, and X. Xu, "Effects of Water Pollution on Human Health and Disease Heterogeneity: A Review," *Front Environ Sci*, vol. 10, p. 880246, Jun. 2022, doi: 10.3389/FENVS.2022.880246/BIBTEX.

[4] P. Jarvis, I. Carra, M. Jafari, and S. J. Judd, "Ceramic vs polymeric membrane implementation for potable water treatment," *Water Res*, vol. 215, May 2022, doi: 10.1016/j.watres.2022.118269.

[5] M. Ağtaş, M. Dilaver, and İ. Koyuncu, "Ceramic membrane overview and applications in textile industry: a review," *Water Science and Technology*, vol. 84, no. 5, pp. 1059–1078, Sep. 2021, doi: 10.2166/WST.2021.290.

[6] "America's Authority in Membrane Treatment."

[7] M. Bat-Amgalan, N. Kano, N. Miyamoto, H. J. Kim, and G. Yunden, "Fabrication and Properties of Adsorptive Ceramic Membrane Made from Kaolin with Addition of Dolomite for Removal of Metal Ions in a Multielement Aqueous System," *ACS Omega*, Oct. 2024, doi: 10.1021/ACSOMEGA.4C06785/ASSET/IMAGES/LARGE/AO4C06785_0020.JPEG.

[8] L. Sawunyama, O. A. Oyewo, M. F. Bopape, and D. C. Onwudiwe, "Fabrication and characterization of low-cost ceramic membranes from coal fly ash and natural sand," *Sustainable Chemistry for the Environment*, vol. 8, p. 100165, Dec. 2024, doi: 10.1016/J.SCENV.2024.100165.

[9] L. Sawunyama, O. C. Olatunde, O. A. Oyewo, M. F. Bopape, and D. C. Onwudiwe, "Application of coal fly ash based ceramic membranes in wastewater treatment: A sustainable alternative to commercial materials," *Heliyon*, vol. 10, no. 2, p. e24344, Jan. 2024, doi: 10.1016/J.HELIYON.2024.E24344.

[10] A. Keshav, S. Saxena, ; A B Soni, and A. Jayapal, "Fabrication of Novel Ceramic Membrane Using Coal Fly Ash Blended with Fuller's Clay for Separation of Technical Lignin," *J Hazard Toxic Radioact Waste*, vol. 29, no. 2, p. 04025006, Apr. 2025, doi: 10.1061/JHTRBP.HZENG-1369.

[11] S. K. Gupta and S. Rani, "Characterisation Of Fly Ash From Thermal Power Plant," *IOSR Journal of Applied Chemistry (IOSR-JAC*, vol. 16, no. 5, pp. 20–24, 2023, doi: 10.9790/5736-1605012024.

[12] Z. ; Zhang *et al.*, “Development of Hydrophobic Coal-Fly-Ash-Based Ceramic Membrane for Vacuum Membrane Distillation,” *Materials 2023, Vol. 16, Page 3153*, vol. 16, no. 8, p. 3153, Apr. 2023, doi: 10.3390/MA16083153.

[13] Marwan Shamo Shekho and Najmaldin Ezaldin Hassan, “A review on techniques for the cleaning of wastewater,” *GSC Advanced Research and Reviews*, vol. 18, no. 1, pp. 118–128, Jan. 2024, doi: 10.30574/gscarr.2024.18.1.0005.

[14] B. J. Singh, A. Chakraborty, and R. Sehgal, “A systematic review of industrial wastewater management: Evaluating challenges and enablers,” *J Environ Manage*, vol. 348, p. 119230, Dec. 2023, doi: 10.1016/J.JENVMAN.2023.119230.

[15] E. O. Ezugbe and S. Rathilal, “Membrane Technologies in Wastewater Treatment: A Review,” *Membranes (Basel)*, vol. 10, no. 5, p. 89, May 2020, doi: 10.3390/MEMBRANES10050089.

[16] M. Klatt, F. Beyer, and J. Einfeldt, “Hospital wastewater treatment and the role of membrane filtration – removal of micropollutants and pathogens: A review,” *Water Science and Technology*, vol. 86, no. 9, pp. 2213–2232, Nov. 2022, doi: 10.2166/WST.2022.321.

[17] M. Ağtaş, M. Dilaver, and İ. Koyuncu, “Ceramic membrane overview and applications in textile industry: a review,” *Water Science and Technology*, vol. 84, no. 5, pp. 1059–1078, Sep. 2021, doi: 10.2166/WST.2021.290.

[18] R. M. Andrade, N. G. Jaques, J. Sousa, R. P. S. Dutra, D. A. MacEdo, and L. F. A. Campos, “Preparation of low-cost ceramic membranes for microfiltration using sugarcane bagasse ash as a pore-forming agent,” *Ceramica*, vol. 65, no. 376, pp. 620–625, 2019, doi: 10.1590/0366-69132019653762696.

[19] S. Dhiman, M. Balakrishnan, V. Naddeo, and N. Ahsan, “Performance of Anaerobic Membrane Bioreactor (AnMBR) with Sugarcane Bagasse Ash-based Ceramic Membrane treating Simulated Low-strength Municipal Wastewater: Effect of Operation Conditions,” *Water Air Soil Pollut*, vol. 234, no. 3, p. 141, Mar. 2023, doi: 10.1007/S11270-023-06173-3.

[20] B. K. Nandi, R. Uppaluri, and M. K. Purkait, “Preparation and characterization of low cost ceramic membranes for micro-filtration applications,” *Appl Clay Sci*, vol. 42, no. 1–2, pp. 102–110, Dec. 2008, doi: 10.1016/J.CLAY.2007.12.001.

[21] L. Sun, Z. Wang, and B. Gao, “Ceramic membranes originated from cost-effective and abundant natural minerals and industrial wastes for broad applications – a review,” 2020, *Desalination Publications*. doi: 10.5004/dwt.2020.25910.

[22] P. Jarvis, I. Carra, M. Jafari, and S. J. Judd, “Ceramic vs polymeric membrane implementation for potable water treatment,” *Water Res*, vol. 215, May 2022, doi: 10.1016/j.watres.2022.118269.

[23] “Membrane filtration technology has become an essential tool for modern...” Accessed: Jun. 23, 2025. [Online]. Available:

https://www.perplexity.ai/search/give-suitable-references-and-a-HfrDOGtfQZm2I6eyViwdUw

[24] N. F. Binti and C. Bahar, “DEVELOPMENT OF ASYMMETRIC POLYETHERSULFONE (PES) MIXED MATRIX MEMBRANE FOR O 2 /N 2 SEPARATION,” 2010.

[25] “Membrane Separation Market Size And Share Report, 2030.” Accessed: Jun. 23, 2025. [Online]. Available: https://www.grandviewresearch.com/industry-analysis/membrane-separation-market

[26] “03 Chap 3 Membrane Preparation Phase Inversion | PDF | Membrane Technology | Evaporation.” Accessed: Jun. 23, 2025. [Online]. Available: https://www.scribd.com/presentation/140845765/03-Chap-3-Membrane-Preparation-Phase-Inversion-1

[27] “Ceramic Membrane Market Size | Industry Report, 2030.” Accessed: Jun. 23, 2025. [Online]. Available: https://www.grandviewresearch.com/industry-analysis/ceramic-membrane-market-report

[28] “Ceramic Membrane Market Size, Share, Trends & Forecast.” Accessed: Jun. 23, 2025. [Online]. Available: https://www.verifiedmarketresearch.com/product/ceramic-membrane-market/

[29] “Ceramic Membranes Market Trends 2025-2035.” Accessed: Jun. 23, 2025. [Online]. Available: https://www.futuremarketinsights.com/reports/ceramic-membranes-market

[30] “Ceramic Membrane Market Size | Industry Report, 2030.” Accessed: Jun. 23, 2025. [Online]. Available: https://www.grandviewresearch.com/industry-analysis/ceramic-membrane-market-report

[31] “Ceramic Membranes and Membrane Processes,” 2007.

[32] “Applications of Ceramic Membrane Technology in the Water and Wastewater Treatment Industry - JIUWU HI-TECH Membrane Technology.” Accessed: Jun. 23, 2025. [Online]. Available: https://www.jiuwumembrane.com/ceramic-membrane-technology-in-the-water.html

[33] R. B. Merlet, M. A. Pizzoccaro-Zilamy, A. Nijmeijer, and L. Winnubst, “Hybrid ceramic membranes for organic solvent nanofiltration: State-of-the-art and challenges,” *J Memb Sci*, vol. 599, p. 117839, Apr. 2020, doi: 10.1016/J.MEMSCI.2020.117839.

[34] A. E. Souza, S. R. Teixeira, G. T. A. Santos, F. B. Costa, and E. Longo, “Reuse of sugarcane bagasse ash (SCBA) to produce ceramic materials,” *J Environ Manage*, vol. 92, no. 10, pp. 2774–2780, Oct. 2011, doi: 10.1016/J.JENVMAN.2011.06.020.

[35] L. Sawunyama, O. C. Olatunde, O. A. Oyewo, M. F. Bopape, and D. C. Onwudiwe, “Application of coal fly ash based ceramic membranes in wastewater treatment: A

sustainable alternative to commercial materials," *Heliyon*, vol. 10, no. 2, p. e24344, Jan. 2024, doi: 10.1016/J.HELIYON.2024.E24344.

[36] H. M. de Oliveira, H. de Lucena Lira, and L. N. de Lima Santana, "Thermal Processing Effects on Biomass Ash Utilization for Ceramic Membrane Fabrication," *Sustainability 2025, Vol. 17, Page 979*, vol. 17, no. 3, p. 979, Jan. 2025, doi: 10.3390/SU17030979.

[37] C. Fernández-Pereira, C. Leiva, Y. Luna-Galiano, L. F. Vilches, and F. Arroyo, "Improved recycling of a gasification fly ash: An integrated waste management approach within the framework of a Circular Economy," *Waste Management*, vol. 187, pp. 31–38, Oct. 2024, doi: 10.1016/j.wasman.2024.06.029.

[38] V. Torres, M. Sadique, and P. Pineda, "Environmental Benefits of Using Activated Sugarcane Bagasse Ash in Cementitious Materials," vol. 4, pp. 723–713, Dec. 2023, doi: 10.29007/GS5Q.

[39] R. M. Andrade, N. G. Jaques, J. Sousa, R. P. S. Dutra, D. A. MacEdo, and L. F. A. Campos, "Preparation of low-cost ceramic membranes for microfiltration using sugarcane bagasse ash as a pore-forming agent," *Ceramica*, vol. 65, no. 376, pp. 620–625, 2019, doi: 10.1590/0366-69132019653762696.

[40] M. T. M. Hussien Hamad, "Optimization study of the adsorption of malachite green removal by MgO nano-composite, nano-bentonite and fungal immobilization on active carbon using response surface methodology and kinetic study," *Environ Sci Eur*, vol. 35, no. 1, Dec. 2023, doi: 10.1186/s12302-023-00728-1.

[41] M. Abewaa, A. Mengistu, T. Takele, J. Fito, and T. Nkambule, "Adsorptive removal of malachite green dye from aqueous solution using Rumex abyssinicus derived activated carbon," *Sci Rep*, vol. 13, no. 1, Dec. 2023, doi: 10.1038/s41598-023-41957-x.

[42] D. Das Pramanik, P. Garg, D. Ganesan, and A. Pramanik, "Removal of malachite green from an aqueous environment using chitosan-xanthan gum coagulation system: A response surface methodology approach," *Journal of Water Process Engineering*, vol. 65, Aug. 2024, doi: 10.1016/j.jwpe.2024.105896.

[43] F. Meng, S. R. Chae, A. Drews, M. Kraume, H. S. Shin, and F. Yang, "Recent advances in membrane bioreactors (MBRs): Membrane fouling and membrane material," *Water Res*, vol. 43, no. 6, pp. 1489–1512, Apr. 2009, doi: 10.1016/J.WATRES.2008.12.044.

[44] Z. He, Z. Lyu, Q. Gu, L. Zhang, and J. Wang, "Ceramic-based membranes for water and wastewater treatment," Oct. 05, 2019, *Elsevier B.V.* doi: 10.1016/j.colsurfa.2019.05.074.

[45] S. K. Hubadillah *et al.*, "Fabrications and applications of low cost ceramic membrane from kaolin: A comprehensive review," *Ceram Int*, vol. 44, no. 5, pp. 4538–4560, Apr. 2018, doi: 10.1016/J.CERAMINT.2017.12.215.

[46] S. N. A. Zulkifli, A. Mustafa, M. H. D. Othman, and S. K. Hubadillah, "Characteristic properties of ceramic membrane derived from fly ash with different loadings and sintering temperature," *Malaysian Journal of Fundamental and Applied Sciences*, vol. 15, no. 3, pp. 414–420, May 2019, doi: 10.11113/MJFAS.V15N3.1225.

[47] M. Rawat and V. K. Bulasara, "Synthesis and characterization of low-cost ceramic membranes from fly ash and kaolin for humic acid separation," *Korean Journal of Chemical Engineering*, vol. 35, no. 3, pp. 725–733, Mar. 2018, doi: 10.1007/S11814-017-0316-6.

[48] C. Cai, W. Sun, S. He, Y. Zhang, and X. Wang, "Ceramic membrane fouling mechanisms and control for water treatment," *Front Environ Sci Eng*, vol. 17, no. 10, pp. 126-, Oct. 2023, doi: 10.1007/S11783-023-1726-9.

[49] E. Zuriaga-Agustí, E. Alventosa-deLara, S. Barredo-Damas, M. I. Alcaina-Miranda, M. I. Iborra-Clar, and J. A. Mendoza-Roca, "Performance of ceramic ultrafiltration membranes and fouling behavior of a dye-polysaccharide binary system," *Water Res*, vol. 54, pp. 199–210, May 2014, doi: 10.1016/j.watres.2014.01.064.

[50] L. Munla, "A Study of Fouling on Ceramic Ultrafiltration Membranes by Model Solutions and Natural Waters," 2013, *University of Waterloo*. Accessed: Jun. 23, 2025. [Online]. Available: http://hdl.handle.net/10012/7618

[51] S. Srivastava, R. Sinha, and D. Roy, "Toxicological effects of malachite green," *Aquatic Toxicology*, vol. 66, no. 3, pp. 319–329, Feb. 2004, doi: 10.1016/j.aquatox.2003.09.008.

[52] G. Certistain, "Material Safety Data Sheet Malachite Green oxalate salt sc-206010 Section 1-CHEMICAL PRODUCT AND COMPANY IDENTIFICATION PRODUCT NAME STATEMENT OF HAZARDOUS NATURE NFPA SUPPLIER Section 2-HAZARDS IDENTIFICATION CHEMWATCH HAZARD RATINGS."

[53] A. Micheal and R. R. Moussa, "Investigating the Economic and Environmental Effect of Integrating Sugarcane Bagasse (SCB) Fibers in Cement Bricks," *Ain Shams Engineering Journal*, vol. 12, no. 3, pp. 3297–3303, Sep. 2021, doi: 10.1016/J.ASEJ.2020.12.012.

[54] M. Ahmaruzzaman, "A review on the utilization of fly ash," *Prog Energy Combust Sci*, vol. 36, no. 3, pp. 327–363, Jun. 2010, doi: 10.1016/j.pecs.2009.11.003.

[55] "Bagasse polluting city, reveals study | Nagpur News - Times of India." Accessed: Jun. 23, 2025. [Online]. Available: https://timesofindia.indiatimes.com/city/nagpur/bagasse-polluting-city-reveals-study/articleshow/47682735.cms

[56] "7 Sustainable Uses of Sugarcane Wastes." Accessed: Jun. 23, 2025. [Online]. Available: https://www.wastex.io/post/sugarcane-waste-uses

[57] S. Subramanian, G. Pande, G. De Weireld, J. M. Giraudon, J. F. Lamonier, and V. S. Batra, “Sugarcane bagasse fly ash as an attractive agro-industry source for VOC removal on porous carbon,” *Ind Crops Prod*, vol. 49, pp. 108–116, Aug. 2013, doi: 10.1016/j.indcrop.2013.04.014.

[58] A. Manrique, K. Clarke, S. Bisesi, F. A. Arosemena, E. S. Coker, and T. Sabo-Attwood, “The Adverse Health Effects of Air Pollution from Sugarcane Burning: A Scoping Review of Observational and Experimental Evidence,” *Environ Health Perspect*, vol. 133, no. 1, p. 016002, Jan. 2025, doi: 10.1289/EHP14456.

[59] “Sustainable Development Goals - Operation Eyesight.” Accessed: Jun. 23, 2025. [Online]. Available: https://operationeyesightindia.org/sustainable-development-goals/?gad_source=1&gad_campaignid=20928237255&gbraid=0AAAAAqqvbtIY4MEEp-KD72hdJgCmFga6o&gclid=Cj0KCQjw097CBhDIARIsAJ3-nxdMF7lnfy4q4Tv3AtIgfGRDK-6PpKuusKTVA5ktqcaghH6OD2PMzEkaAsbiEALw_wcB

[60] L. Sawunyama, O. A. Oyewo, M. F. Bopape, and D. C. Onwudiwe, “Fabrication and characterization of low-cost ceramic membranes from coal fly ash and natural sand,” *Sustainable Chemistry for the Environment*, vol. 8, Dec. 2024, doi: 10.1016/J.SCENV.2024.100165.

[61] T. Neamhom, “Use of Agricultural Residues to Remove Iron from Groundwater in Modified Airlift Aerator,” *Environ Nat Resour J*, vol. 17, no. 3, pp. 58–67, Apr. 2019, doi: 10.32526/ENNRJ.17.3.2019.23.

[62] X. Fan, L. Deng, K. Li, H. Lu, R. Wang, and W. Li, “Adsorption of malachite green in aqueous solution using sugarcane bagasse-barium carbonate composite,” *Colloid Interface Sci Commun*, vol. 44, p. 100485, Sep. 2021, doi: 10.1016/J.COLCOM.2021.100485.

[63] D. Ariani, N. H. Aprilita, and A. Kuncaka, “Adsorption of Malachite Green and Methyl Violet 2B with Phthalate-Functionalized Sugarcane Bagasse,” *BIMIPA*, vol. 25, no. 1, pp. 66–79, Jan. 2018, Accessed: Jun. 23, 2025. [Online]. Available: https://jurnal.ugm.ac.id/bimipa/article/view/26973

[64] L. Sawunyama, O. C. Olatunde, O. A. Oyewo, M. F. Bopape, and D. C. Onwudiwe, “Application of coal fly ash based ceramic membranes in wastewater treatment: A sustainable alternative to commercial materials,” *Heliyon*, vol. 10, no. 2, p. e24344, Jan. 2024, doi: 10.1016/J.HELIYON.2024.E24344.

[65] L. Sawunyama, O. A. Oyewo, M. F. Bopape, and D. C. Onwudiwe, “Fabrication and characterization of low-cost ceramic membranes from coal fly ash and natural sand,” *Sustainable Chemistry for the Environment*, vol. 8, Dec. 2024, doi: 10.1016/J.SCENV.2024.100165.

[66] P. K. Ramteke, A. P. Rathod, S. M. Kodape, and S. S. Sonawane, “Development and evaluation of environmentally sustainable cenosphere ceramic membrane for the

efficient separation of methylene blue dye," *Chemical Papers*, Jan. 2024, doi: 10.1007/s11696-024-03782-y.

[67] K. Singh, A. Kumar, A. K. Singh, and A. Agarwal, "Fly ash and TiO2 modified fly ash as adsorbing materials for effective removal of methylene blue and malachite green from aqueous solutions," *Journal of the Indian Chemical Society*, vol. 100, no. 3, p. 100942, Mar. 2023, doi: 10.1016/J.JICS.2023.100942.

[68] N. Akhtar *et al.*, "Decolorization of multicomponent dye-laden wastewater by modified waste fly ash: a parametric analysis for an anionic and cationic combination of dyes," *Environmental Science and Pollution Research*, vol. 30, no. 31, pp. 77165–77180, Jul. 2023, doi: 10.1007/S11356-023-27671-1/TABLES/6.

[69] D. Almasri *et al.*, "A novel, low-cost clay ceramic membrane for the separation of oil-water emulsions," *Sci Rep*, vol. 15, no. 1, Dec. 2025, doi: 10.1038/s41598-025-99143-0.

[70] Y. Manawi, V. Kochkodan, E. Mahmoudi, D. J. Johnson, A. W. Mohammad, and M. A. Atieh, "Characterization and Separation Performance of a Novel Polyethersulfone Membrane Blended with Acacia Gum," *Sci Rep*, vol. 7, no. 1, Dec. 2017, doi: 10.1038/s41598-017-14735-9.

[71] J. Saikia, S. Sarmah, J. J. Bora, B. Das, and R. L. Goswamee, "Preparation and characterization of low cost flat ceramic membranes from easily available potters' clay for dye separation," *Bulletin of Materials Science*, vol. 42, no. 3, Jun. 2019, doi: 10.1007/S12034-019-1767-7.

[72] R. Vinoth Kumar, A. Kumar Ghoshal, and G. Pugazhenthi, "Elaboration of novel tubular ceramic membrane from inexpensive raw materials by extrusion method and its performance in microfiltration of synthetic oily wastewater treatment," *J Memb Sci*, vol. 490, pp. 92–102, Sep. 2015, doi: 10.1016/J.MEMSCI.2015.04.066.

[73] "XRD diffraction patterns of the raw materials (a) kaolin, (b)... | Download Scientific Diagram." Accessed: Jun. 28, 2025. [Online]. Available: https://www.researchgate.net/figure/XRD-diffraction-patterns-of-the-raw-materials-a-kaolin-b-bentonite-and-c_fig1_360287365

[74] J. Zhao *et al.*, "Fabrication of porous Al2TiO5-Al2O3 ceramics using Al2O3 hollow spheres coated with TiO2 sol," *Ceram Int*, vol. 48, no. 19, pp. 27349–27359, Oct. 2022, doi: 10.1016/J.CERAMINT.2022.05.155.

[75] J. Zhao *et al.*, "Fabrication of porous Al2TiO5-Al2O3 ceramics using Al2O3 hollow spheres coated with TiO2 sol," *Ceram Int*, vol. 48, no. 19, pp. 27349–27359, Oct. 2022, doi: 10.1016/J.CERAMINT.2022.05.155.

[76] M. Chaudhary, S. Rawat, and A. Maiti, "Defluoridation by Bare Nanoadsorbents, Nanocomposites, and Nanoadsorbent Loaded Mixed Matrix Membranes," *Separation & Purification Reviews*, vol. 52, no. 2, pp. 135–153, Apr. 2023, doi: 10.1080/15422119.2022.2045610.